Recent advances in modeling and simulation of thermoelectric power generation

Ding Luo[a], Zerui Liu[a], Yuying Yan[b], Ying Li[b], Ruochen Wang[c], Lulu Zhang[a], Xuelin Yang[a,*]

[a] Collaborative Innovation Center for Microgrid of New Energy, College of Electrical Engineering & New Energy, China Three Gorges University, Yichang, China

[b] Faculty of Engineering, University of Nottingham, Nottingham, UK

[c] School of Automobile and Traffic Engineering, Jiangsu University, Zhenjiang, China

Corresponding authors: *Xuelin Yang, xlyang@ctgu.edu.cn

Abstract: Thermoelectric power generation is a renewable energy conversion technology that can directly convert heat into electricity. In recent years, a great number of theoretical models have been established to predict and optimize the performance of both thermoelectric generators and thermoelectric generator systems. In this work, a comprehensive review of theoretical models is given with a specific focus on the different modeling approaches and different application scenarios. Firstly, the basic principles of theoretical models of the thermoelectric generator are presented, including the thermal resistance model, thermal-electric numerical model, and analogy model. Then, the theoretical models of the thermoelectric generator system are reviewed in detail, including the thermal resistance-based analytical model, computational fluid dynamics models, and fluid-thermal-electric multiphysics field coupled numerical model. The methods to improve the accuracy of theoretical models are also discussed. Furthermore, the transient thermal-electric numerical model of the thermoelectric generator and the transient fluid-thermal-electric multiphysics field coupled numerical model of the thermoelectric generator system are introduced, which can take into account the dynamic characteristics of the heat source, and may remain a hot research field in the upcoming years. Generally, thermal resistance models can quickly obtain the performance of the thermoelectric generator and thermoelectric generator system under different parameters, but suffer from relatively large errors; while it is the opposite for numerical models. To design a comprehensive thermoelectric generator system for practical application, it is suggested to combine the advantages of different models, to shorten the development time and ensure optimal performance at the same time.

Keywords: Thermoelectric generator; Theoretical model; Thermal resistance; Numerical model; Transient

Nomenclature

Symbols

A	Area, m^2
c	Specific heat, $J\cdot kg^{-1}\cdot K^{-1}$
$\vec{E}$	Electric field density vector, $V\cdot m^{-2}$
H	Height, m
h	Heat transfer coefficient, $W\cdot m^{-2}\cdot K^{-1}$
I	Current, A
$\vec{J}$	Current density vector, $A\cdot m^{-2}$
$\dot{m}$	Mass flow rate, $kg\cdot s^{-1}$
N	Number
Nu	Nusselt number
P	Power, W
Pr	Prandtl number
Q	Heat, W
$\dot{q}$	Heat flux, $W\cdot m^{-2}$
R	Resistance, Ω or $K\cdot W^{-1}$
Re	Reynolds number
T	Temperature, K
t	Time, s
U	Voltage, V
v	Velocity, $m\cdot s^{-1}$
$\vec{v}$	Velocity vector, $m\cdot s^{-1}$
x	x-dimension

Greek symbols

α	Seebeck coefficient, $V\cdot K^{-1}$
λ	Thermal conductivity, $W\cdot m^{-1}\cdot K^{-1}$
σ	Electrical conductivity, $S\cdot m^{-1}$
η	Conversion efficiency
ϕ	Electrical potential, V
ρ	Density, $kg\cdot m^{-3}$
μ	Dynamic viscosity, Pa·s
δ	Thickness, m

Subscripts

c	Cold side
ce	Ceramic plate
co	Copper electrode
ex	Exhaust gas
ext	External environment
h	Hot side
hp	Heat pipe
in	Internal resistance
L	Load resistance
leg	thermoelectric leg
m	Material name
n	n-type thermoelectric leg
p	p-type thermoelectric leg
pn	Thermoelectric couple
sink	Heat sink
wa	Water

Abbreviations

CFD	Computational fluid dynamics
FDM	Finite difference method
FEM	Finite element method
FVM	Finite volume method
TEG	Thermoelectric generator
UDF	User defined function

1. Introduction

Due to the tremendous use of fossil fuels, energy shortage and environmentally harmful emissions have become global problems in recent years, and many countries have issued policies to reduce the use of fossil energy and promote the development of green alternative energy techniques. One feasible way is to convert the kinetic energy or potential energy produced in nature into electrical energy, such as hydropower, wind power, and tidal power stations, which usually need to convert the energy into mechanical energy and then drive the generator to produce electricity. Another way is to convert solar energy or thermal energy directly into electricity by using some particular semiconductors, such as photovoltaic and thermoelectric power generation, which do not need any intermediate energy conversion unit. All the green alternative energy technologies mentioned, except for thermoelectric technology, are more or less weather dependent. Besides, thermoelectric power generation was regarded as a promising alternative energy conversion technology, owing to its unparalleled merits of no moving parts, no pollution, silent operation, no maintenance costs, and long service life [1-3].

In practical application, a thermoelectric generator (TEG) module is used as the basic power generation unit, which combines heat source, cooling source, and heat exchanger devices into a TEG system, and then generates electricity to supply power for electronic devices. According to the different heat sources, the TEG system can be classified into two types: the TEG system for fluid waste heat recovery and the TEG system directly contacted with a heat source. The TEG system for fluid waste heat recovery is generally used to recover the waste heat contained in thermal fluids, like automobile exhaust waste heat and industrial waste heat. The corresponding automotive TEG system [4, 5] and industry waste-heat-recovery TEG system [6, 7] prototypes have been developed to recycle the waste heat and reduce energy consumption. As for the TEG system directly contacted with a heat source, the heat source directly provides a high temperature or heat flux to the hot side of the TEG modules, without the need for the heat exchanger to collect heat from thermal fluids. Using the decay energy of radioactive elements as a heat source, the radioisotope TEG system [8, 9] has been widely used in the spacecraft power supply. Due to the low requirement of power intensity, thermoelectric generators can also be used to harvest body heat and supply power for wearable devices [10]. In off-grid areas and emergencies, the stove-powered TEG system was an effective approach to obtaining electricity [11, 12]. Unlike TEG systems applied in fluid waste heat recovery, the heat source of these TEG systems is directly imposed on the hot side surfaces of the TEG module or the plates contacted with the TEG module.

The behavior of TEG systems is generally evaluated by the output characteristic parameters of output power and conversion efficiency, and great progress in the performance of TEG systems has been made in recent years. However, the wide commercialization of TEG technology is still limited by the low conversion efficiency of TEG systems. To further improve the heat-to-electricity conversion efficiency, both the advancement of thermoelectric materials and the optimization of thermoelectric devices need to be conducted. At present, the figure of merit (ZT) of most thermoelectric materials ranges from 1 to 1.6, while the potential commercial application of waste heat recovery needs ZT to reach 2.0 [13]. The threshold of ZT = 2.0 may be broken through shortly, thanks to the development of modern synthesis and characteristic technologies, like nanostructured thermoelectric materials [14]. Besides the exploration of high-performance thermoelectric materials, the structural optimization approaches of both TEGs and TEG systems can also improve the output power and conversion efficiency. For the scenario of TEGs, segmented thermoelectric unicouples [15, 16], two-stage design [17], and asymmetric thermoelectric devices [18] were commonly used optimization methods to improve the efficiency and reduce the parasitic power losses. For the scenario of the TEG system applied in fluid waste heat recovery, an additional heat exchanger was required to deliver heat from thermal fluids to TEGs, and thus, many researchers [19, 20] have made great efforts to optimize the heat transfer performance of heat exchanger.

Theoretical models are the premise to predict the performance and conduct the structure optimizations of TEGs and TEG systems. Compared with experimental methods, model predictions can save a lot of time and money, especially when several parameters need to be optimized. Consequently, reasonable models need to be developed to predict the performance of TEGs and TEG systems. As the heat flows through the TEG, the temperature difference will drive holes in p-type thermoelectric materials and electrons in n-type thermoelectric materials moving from hot side to cold side, so that a Seebeck voltage is generated, as shown in Fig. 1 (a). At the same time, the cold side interface of carrier accumulation will release heat, and the hot side interface of carrier dissipation will absorb heat, as a result of the Peltier effect; Because of the temperature gradient of thermoelectric semiconductors, it will be accompanied by the generation of Thomson heat; As the electric current flows through thermoelectric semiconductors, metal electrodes, and load resistance, it will be accompanied by the generation of Joule heat. Based on these fundamental principles, various TEG models [21, 22] have been proposed to evaluate the performance of a specific TEG design and optimize its structure.

When TEGs are adopted in a specific field to recover waste heat or supply power, a more complex heat transfer process is involved. Compared with TEGs, a Fourier heat conduction process from the heat source to TEGs was involved in the TEG system directly contacted with a heat source. And the performance of this TEG system can be predicted by adding additional heat transfer conservation equations into the theoretical models of TEG. However, the situation of the TEG system for fluid waste heat recovery is quite different and more complex. Taking the waste heat recovery from exhaust gases as an example, the heat is first absorbed by the heat exchanger in the form of conjugate heat transfer, then transferred from the heat exchanger to TEGs and heat sink, and finally taken away by the coolant, as shown in Fig. 1(b). The intricate fluid flow and heat transfer process complicate the modeling of TEG systems applied in fluid waste heat recovery [23]. Researchers [24, 25] have been trying to establish a comprehensive model to accurately predict the performance of fluid-based TEG systems.

On the other hand, the heat source of both direct-contact and fluid-based TEG systems varied with different working conditions, and was time-dependent in practical application, for example, the heat flux produced by flame was not static in the stove-powered TEG system; both exhaust temperature and exhaust mass flow rate changed with vehicle speed in the automotive TEG system. Hence, both the TEG model and the TEG system model should be extended from a steady state to a transient state. Challenges surrounding the modeling of TEG systems call for studies to address them.

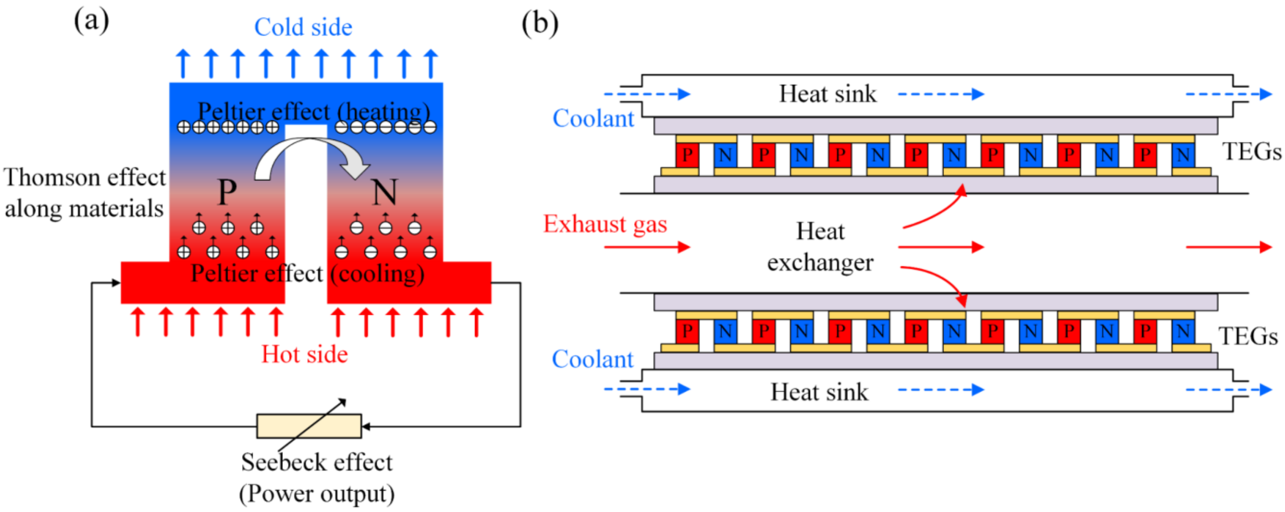

Fig. 1. Fundamental theories of (a) TEG and (b) TEG system (e.g. exhaust waste heat recovery).

This work aims to carry out a comprehensive review of recent advances in modeling for TEGs and TEG systems. The interior parameter transport characteristics between thermal and electric variables are first introduced, and then various theoretical models regarding TEGs proposed in recent literature are reviewed in Section 2. Section 3 describes the theoretical models of TEG systems from one dimension to three dimensions, from a simplified model to a comprehensive model, and from a steady state to a transient state. Section 4 elaborates on the recommendations for the theoretical analysis of thermoelectric power generation devices, including the methods to improve the accuracy of model results and the proper use of models in different applications. This work ends with a concluding remark.

2. Theoretical models of thermoelectric generators

In practical application, the TEG module is the basic power source to convert heat energy into electric energy, which is composed of a series of TEG units, as shown in Fig. 2. A single TEG unit consists of a p-type thermoelectric leg, an n-type thermoelectric leg, copper electrodes, and two ceramic plates. A TEG module can be regarded as a series of TEG units. Therefore, researchers usually take a single TEG unit as the research object to establish the theoretical model of TEGs and analyze their performance. In this section, the fundamental principles of TEGs are introduced firstly, and then the recent development of TEG theoretical models is reviewed from one dimension to three dimensions, from TEG unit to TEG module, and from a steady state to a transient state. Finally, the comparative analysis and comment on different models are provided in Section 2.5.

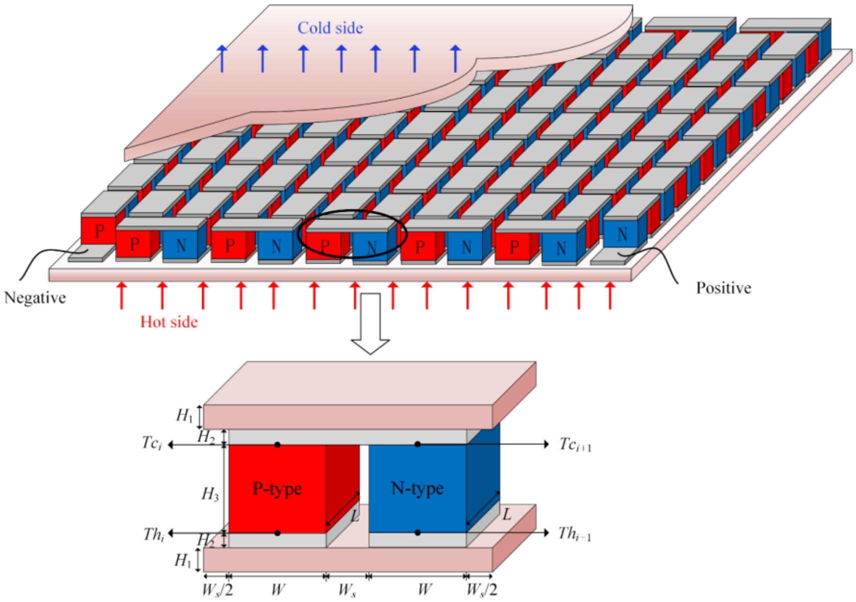

Fig. 2. Topological relationship between TEG module and TEG unit [26].

2.1 Fundamental principles of thermoelectric generators

The thermoelectric coupling effect includes the Seebeck effect, Peltier effect, and Thomson effect. Based on the Seebeck effect, the Seebeck voltage is determined, which equals the product of the Seebeck coefficient (α) and temperature difference (ΔT). Due to the Peltier effect, when the carriers of thermoelectric materials are transferred from the hot end to the cold end, the side of carrier accumulation will release heat, while the side of carrier dissipation will absorb heat. This endothermic and exothermic heat is called hot side Peltier heat and cold side Peltier heat respectively, which is equal to the product of Seebeck coefficient (α), current (I), and absolute temperature (T). Due to the Thomson effect, when the current direction is consistent with the temperature gradient direction, thermoelectric semiconductors will release heat, and vice versa. In addition to these three thermoelectric coupling effects, the Fourier heat conduction effect and Joule effect also occur. The amount of heat transfer from the hot end to the cold end is equal to Fourier heat. Joule heat is generated when the current passes through the thermoelectric semiconductor. Generally, the Fourier heat is the highest, followed by the hot side Peltier heat, cold side Peltier heat, Joule heat, and Thomson heat.

Furthermore, thermoelectric material properties are the necessary data to predict the TEG performance, including Seebeck coefficient (α), thermal conductivity (λ), and electric conductivity (σ). The thermoelectric properties establish the figure of merit (ZT), $ZT = \alpha^2 \sigma T / \lambda$, which characterizes the performance of thermoelectric material. In essence, the high Seebeck coefficient (α) helps to maximize the heat-to-electric conversion efficiency, the high electric conductivity (σ) can minimize the internal resistance and reduce the Joule heat, and the low thermal conductivity (λ) helps to maintain a high-temperature difference (ΔT) on both ends of thermoelectric semiconductors [27]. Besides, thermoelectric properties are highly temperature-dependent. Chen et al. [28] conducted a comprehensive analysis of the TEG performance with constant and temperature-dependent properties and reported that the consideration of temperature dependence of thermoelectric materials can provide more realistic predictions. Consequently, the temperature-dependent material properties should be considered in the modeling process.

Based on the above basic principles, a reasonable theoretical TEG model can be established. At present, there are three main modeling methods, including the thermal resistance model, numerical model, and analogy model. In the following sections, recent developments of the three models are reviewed respectively.

2.2 Thermal resistance models

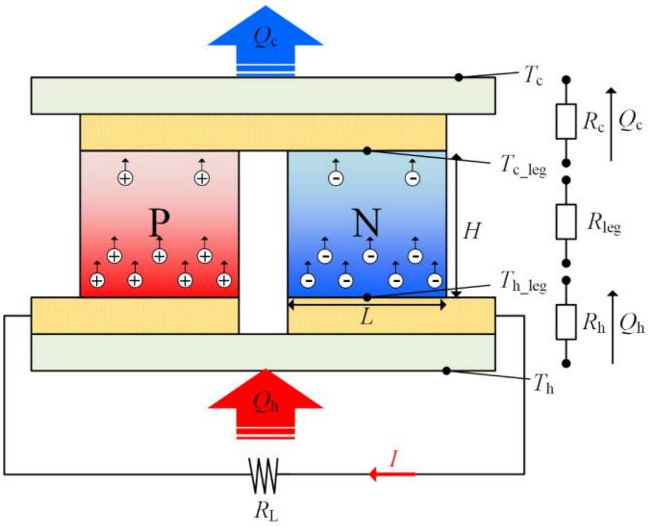

Fig. 3. Schematic diagram of the thermal resistance model of the TEG unit.

The thermal resistance model is based on a global energy balance, assuming that Thomson heat and ambient convection heat transfer are negligible, and Joule heat is uniformly heated at both ends of TEG. The TEG output power is considered as the difference between the hot end heat flux and the cold end heat flux. The schematic diagram of the thermal resistance model is shown in Fig. 3. The average temperature of different cross sections is taken as the actual working temperature to carry out the calculation of TEG output performance. However, the thermal resistance model can only consider the heat transfer from the hot side to the cold side, so it is a one-dimensional model and can not be extended to higher dimensions.

2.2.1 The simplified model

In the simplified thermal resistance models [29, 30], the temperature of the hot side ceramic plate (T_h) and the temperature of the cold side ceramic plate (T_c) are respectively used as the hot side and cold side working temperatures of p-type and n-type thermoelectric legs. Furthermore, the hot side flux can be expressed as:

$$Q_\mathrm{h} = \alpha_\mathrm{pn} I T_\mathrm{h} + \frac{T_\mathrm{h} - T_\mathrm{c}}{R_\mathrm{leg}} - \frac{1}{2} I^2 R_\mathrm{in} \tag{1}$$

where, I is the electric current, R_leg is the thermal resistance of thermoelectric legs, and R_in is the internal resistance of thermoelectric legs.

Also, the cold side flux can be written as:

$$Q_\mathrm{c} = \alpha_\mathrm{pn} I T_\mathrm{c} + \frac{T_\mathrm{h} - T_\mathrm{c}}{R_\mathrm{leg}} + \frac{1}{2} I^2 R_\mathrm{in} \tag{2}$$

with

$$\alpha_\mathrm{pn} = \alpha_\mathrm{p} - \alpha_\mathrm{n} \tag{3}$$

$$R_\mathrm{leg} = \frac{H_\mathrm{leg}}{\left(\lambda_\mathrm{p} + \lambda_\mathrm{n}\right) A_\mathrm{leg}} \tag{4}$$

$$R_\mathrm{in} = \left(\sigma_\mathrm{p}^{-1} + \sigma_\mathrm{n}^{-1}\right) \frac{H_\mathrm{leg}}{A_\mathrm{leg}} \tag{5}$$

in which, H_leg and A_leg are the height and cross-sectional area of thermoelectric legs, respectively. Here, the size of the p-type thermoelectric leg is assumed to be equal to that of the n-type thermoelectric leg. σ^{-1} is the electric resistivity. Subscripts p and n denote p-type and n-type thermoelectric legs, respectively.

The output power of the TEG unit is obtained by subtracting Eq. (1) from Eq. (2):

$$P = Q_\mathrm{h} - Q_\mathrm{c} = \alpha_\mathrm{pn} I \left(T_\mathrm{h} - T_\mathrm{c}\right) - I^2 R_\mathrm{in} \tag{6}$$

The electric current can be expressed as:

$$I = \frac{\left(T_{\mathrm{h}} - T_{\mathrm{c}}\right)\alpha_{\mathrm{pn}}}{R_{\mathrm{in}} + R_{\mathrm{L}}} \tag{7}$$

where R_{L} is the external resistance.

Combining Eqs (1)-(2) and (6)-(7), there are four equations with four unknowns of P, Q_{h}, Q_{c}, and I, and finally, the output power (P) is obtained under the given thermoelectric material properties, geometrical features of thermoelectric legs, and load resistance. Besides, the conversion efficiency of the TEG unit is defined as:

$$\eta = \frac{P}{Q_{\mathrm{h}}} \tag{8}$$

Furthermore, the thermal resistance model is easy to be extended from TEG unit to TEG module, by replacing Eqs (3)-(5) with

$$\alpha_{\mathrm{pn}} = N\left(\alpha_{\mathrm{p}} - \alpha_{\mathrm{n}}\right) \tag{9}$$

$$R_{\mathrm{leg}} = \frac{H_{\mathrm{leg}}}{N\left(\lambda_{\mathrm{p}} + \lambda_{\mathrm{n}}\right)A_{\mathrm{leg}}} \tag{10}$$

$$R_{\mathrm{in}} = N\left(\sigma_{\mathrm{p}}^{-1} + \sigma_{\mathrm{n}}^{-1}\right)\frac{H_{\mathrm{leg}}}{A_{\mathrm{leg}}} \tag{11}$$

where N is the number of TEG units. In essence, the Seebeck voltage of the TEG module is equivalent to the sum of Seebeck voltages of several TEG units, and TEG units are connected in parallel thermally and in series electrically.

Based on this model, Hsu et al. [30] proposed an effective Seebeck coefficient for the TEG module. According to the experimental results, the output power (P) is taken as the known variable and the Seebeck coefficient (α_{pn}) as the unknown variable, and the Seebeck coefficient (α_{pn}) under different working temperatures is obtained. The manufacturers of TEG modules usually do not provide customers with material properties or overestimate the given data. Their research provides an effective way for engineers to obtain material data by themselves. The authors in [31, 32] extended the model from a conventional TEG module to a two-stage TEG design and optimized the performance of the two-stage TEG module by using the simplified thermal resistance model.

2.2.2 The improved thermal resistance model

In practical situations, the temperature of the hot junction of thermoelectric legs is lower than the heat source temperature, and the temperature of the cold junction of thermoelectric legs is higher than the cooling source temperature, rendering the overestimation of temperature difference in the simplified thermal resistance model. Consequently, the simplified thermal resistance model may overestimate the TEG output performance. Besides, the Seebeck coefficient, thermal conductivity, and electric resistivity of thermoelectric materials are highly temperature-dependent, and ignoring the temperature dependence may lead to additional errors. Considering these factors, an improved thermal resistance model was proposed in [25, 33], in which, the hot side and cold side heat flux were defined as:

$$Q_{\mathrm{h}} = \bar{\alpha}_{\mathrm{pn}} I T_{\mathrm{h\_leg}} + \frac{T_{\mathrm{h\_leg}} - T_{\mathrm{c\_leg}}}{\bar{R}_{\mathrm{leg}}} - \frac{1}{2} I^2 \bar{R}_{\mathrm{in}} \tag{12}$$

$$Q_{\mathrm{c}} = \bar{\alpha}_{\mathrm{pn}} I T_{\mathrm{c\_leg}} + \frac{T_{\mathrm{h\_leg}} - T_{\mathrm{c\_leg}}}{\bar{R}_{\mathrm{leg}}} + \frac{1}{2} I^2 \bar{R}_{\mathrm{in}} \tag{13}$$

where, $T_{\mathrm{h\_leg}}$ and $T_{\mathrm{c\_leg}}$ are the hot junction and cold junction temperature of thermoelectric legs, respectively; $\bar{\alpha}_{\mathrm{pn}}$, $\bar{R}_{\mathrm{leg}}$, and $\bar{R}_{\mathrm{in}}$ are the average Seebeck coefficient, the average thermal resistance, and the average internal resistance of the TEG unit, respectively.

When the heat is transferred from the heat source to the hot junction of thermoelectric legs and from the cold junction of thermoelectric legs to the cooling source, Q_{h} and Q_{c} can also be expressed as:

$$Q_{\mathrm{h}} = \frac{T_{\mathrm{h}} - T_{\mathrm{h\_leg}}}{R_{\mathrm{h}}} \tag{14}$$

$$Q_{\mathrm{c}} = \frac{T_{\mathrm{c\_leg}} - T_{\mathrm{c}}}{R_{\mathrm{c}}} \tag{15}$$

where R_{h} and R_{c} are the overall thermal resistance of the hot side and the cold side, respectively. R_{h} and R_{c} are defined as:

$$R_{\mathrm{h}} = R_{\mathrm{c}} = R_{\mathrm{ce}} + R_{\mathrm{co}} \tag{16}$$

with

$$R_{\mathrm{ce/co}} = \frac{H_{\mathrm{ce/co}}}{\lambda_{\mathrm{ce/co}} A_{\mathrm{ce/co}}} \tag{17}$$

where, R_{ce} (R_{co}), H_{ce} (H_{co}), λ_{ce} (λ_{co}), and A_{ce} (A_{co}) are the conductive thermal resistance, height, thermal conductivity, and cross-sectional area of ceramic plate (copper electrodes), respectively.

The output power of the TEG unit can be derived by:

$$P = Q_{\mathrm{h}} - Q_{\mathrm{c}} = \bar{\alpha}_{\mathrm{pn}} I \left(T_{\mathrm{h\_leg}} - T_{\mathrm{c\_leg}} \right) - I^2 \bar{R}_{\mathrm{in}} \tag{18}$$

where

$$I = \frac{\left(T_{\mathrm{h\_leg}} - T_{\mathrm{c\_leg}}\right)\bar{\alpha}_{\mathrm{pn}}}{\bar{R}_{\mathrm{in}} + R_{\mathrm{L}}} \tag{19}$$

The average Seebeck coefficient ($\bar{\alpha}_{\mathrm{pn}}$), average thermal resistance ($\bar{R}_{\mathrm{leg}}$), and average internal resistance ($\bar{R}_{\mathrm{in}}$) of TEG unit can be expressed as:

$$\bar{\alpha}_{\mathrm{pn}} = \bar{\alpha}_{\mathrm{p}} - \bar{\alpha}_{\mathrm{n}} \tag{20}$$

$$\bar{R}_{\mathrm{leg}} = \frac{H_{\mathrm{leg}}}{\left(\bar{\lambda}_{\mathrm{p}} + \bar{\lambda}_{\mathrm{n}}\right)A_{\mathrm{leg}}} \tag{21}$$

$$\bar{R}_{\mathrm{in}} = \left(\bar{\sigma}_{\mathrm{p}}^{-1} + \bar{\sigma}_{\mathrm{n}}^{-1}\right)\frac{H_{\mathrm{leg}}}{A_{\mathrm{leg}}} \tag{22}$$

with

$$T_{\mathrm{ave}} = \frac{T_{\mathrm{h\_leg}} + T_{\mathrm{c\_leg}}}{2} \tag{23}$$

$$\bar{\alpha}_{\mathrm{p/n}} = \frac{\alpha_{\mathrm{p/n}}(T_{\mathrm{h\_leg}}) + \alpha_{\mathrm{p/n}}(T_{\mathrm{c\_leg}}) + 2\alpha_{\mathrm{p/n}}(T_{\mathrm{ave}})}{4} \tag{24}$$

$$\bar{\lambda}_{\mathrm{p/n}} = \frac{\lambda_{\mathrm{p/n}}(T_{\mathrm{h\_leg}}) + \lambda_{\mathrm{p/n}}(T_{\mathrm{c\_leg}}) + 2\lambda_{\mathrm{p/n}}(T_{\mathrm{ave}})}{4} \tag{25}$$

$$\bar{\sigma}_{\mathrm{p/n}}^{-1} = \frac{\sigma_{\mathrm{p/n}}^{-1}(T_{\mathrm{h\_leg}}) + \sigma_{\mathrm{p/n}}^{-1}(T_{\mathrm{c\_leg}}) + 2\sigma_{\mathrm{p/n}}^{-1}(T_{\mathrm{ave}})}{4} \tag{26}$$

where $\alpha_{\mathrm{p/n}}(T)$, $\lambda_{\mathrm{p/n}}(T)$, and $\sigma_{\mathrm{p/n}}^{-1}\left(T\right)$ are the temperature-dependent Seebeck coefficient, thermal conductivity, and electric resistivity of p/n-type thermoelectric materials.

Combining Eqs (12)-(15) and (18)-(19), there are six equations with six unknowns of Q_{h}, Q_{c}, $T_{\mathrm{h\_leg}}$, $T_{\mathrm{c\_leg}}$, P, and I. However, the $\bar{\alpha}_{\mathrm{pn}}$, $\bar{R}_{\mathrm{leg}}$, and $\bar{R}_{\mathrm{in}}$ are unknown in advance with the unknows of $T_{\mathrm{h\_leg}}$ and $T_{\mathrm{c\_leg}}$. The authors in Refs [25, 33] proposed an iterative calculation method to solve this problem, as shown in Fig. 4. The heat source temperature (T_{h}) and the cooling source temperature (T_{c}) are used as the initial values of $T_{\mathrm{h\_leg}}$ and $T_{\mathrm{c\_leg}}$, and then the updated values are put back into the calculation until tolerance is satisfied.

Similarly, the improved thermal resistance model can be extended from the TEG unit to the TEG module by using the substitution method like from Eqs (3)-(5) to Eqs (9)-(11). Based on the improved thermal resistance model, Fan et al. [33] conducted a comprehensive optimization of the ratio of the thermoelectric leg length and cross-sectional area of the TEG unit; The effect of leg length and cross-sectional area on the maximum output power and maximum power density was also studied in their research. Ignoring the temperature dependence, the authors in Ref. [34] proposed some optimal design methods for the TEG module by analyzing the η- R_{leg}^{-1} characteristic curves under different conditions. For the special structures of TEG devices, Liang et al. [35] and Zhang et al. [16] respectively utilized the improved thermal resistance model to predict the performance of the two-stage TEG module and the segmented TEG unit, and studied the influence of different structural parameters on the output power and conversion efficiency; The basic optimization design principles of these two structures can be found in their researches.

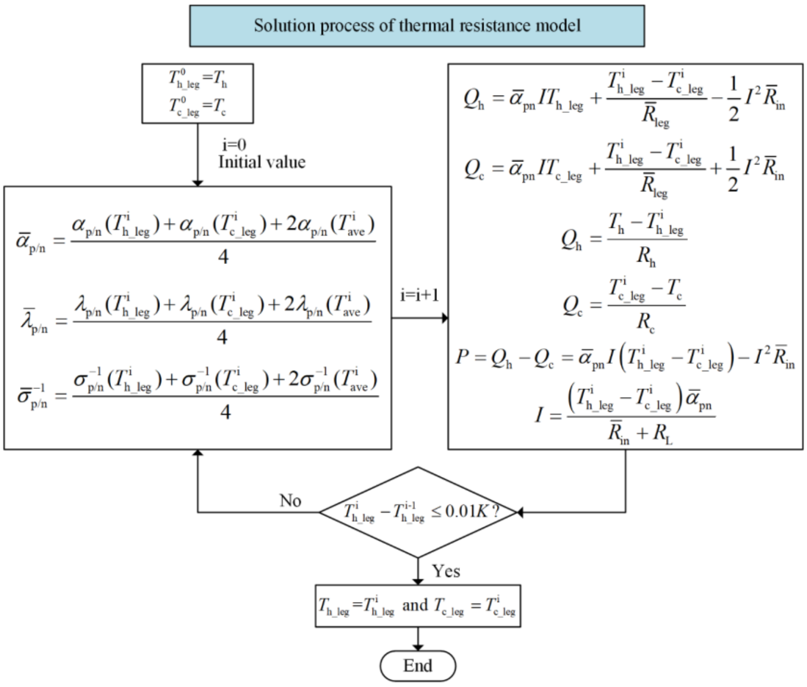

Fig. 4. Solution process of the improved thermal resistance model [25].

As for the transient modeling, few researchers use the thermal resistance model to predict the dynamic performance of TEG, because the transient heat transfer involves the transient change of internal energy, which can not be expressed by thermal resistance. Under the dynamic temperature inputs of T_{h} and T_{c}, the corresponding dynamic output power and conversion efficiency of TEG can be predicted based on the temperature data of different discrete time points. However, in practical situations, the temperature change is continuous. Accordingly, the dynamic performance prediction through a thermal resistance model will further amplify the model error.

2.3 Numerical models

The numerical model is based on the partial differential equations of energy conservation and electric field conservation. Combined with boundary conditions, the partial differential equations can be solved via numerical methods, and the finite difference method (FDM), finite element method (FEM), and finite volume method (FVM) are commonly used numerical approaches. For this reason, numerical analysis software programs such as ANSYS [36, 37] and COMSOL Multiphysics [38, 39] have been widely used to conduct numerical simulations of TEG devices. Generally, the numerical model can take into account all the factors in the actual situation, including the Seebeck effect, Peltier effect, Thomson effect, Joule effect, Fourier heat conduction, electric current flow, heat loss, etc., which is the most reasonable theoretical model to predict the performance of TEG devices. In addition, considering the change of transient internal energy, the numerical model can be extended from a steady state to a transient state.

2.3.1 One-dimensional steady-state numerical model

The governing equations of the TEG numerical model can be divided into three parts: p/n-type thermoelectric legs, copper electrodes, and ceramic plates. In a one-dimensional steady-state numerical model [40-42], the energy conservation of p/n-type thermoelectric legs can be described as:

$$\lambda_{\mathrm{p}}(T)\frac{d^2T}{dx^2} = -\sigma_{\mathrm{p}}^{-1}(T)\vec{J}^2 + \alpha_{\mathrm{p}}(T)\vec{J}\frac{dT}{dx} \tag{27}$$

$$\lambda_{\mathrm{n}}(T)\frac{d^2T}{dx^2} = -\sigma_{\mathrm{n}}^{-1}(T)\vec{J}^2 + \alpha_{\mathrm{n}}(T)\vec{J}\frac{dT}{dx} \tag{28}$$

where, x represents the direction of heat transfer, dx is the infinitesimal element, and $\vec{J}$ is the current density vector. The first term on the left hand denotes the Fourier heat conduction, the first term on the right hand represents the Joule heat, and the second term on the right hand represents the Thomson heat along thermoelectric legs or Peltier heat on junctions.

In the regions of copper electrodes or solder layers, the energy conservation equation can be expressed as:

$$\lambda_{\mathrm{co}}\frac{d^2T}{dx^2} = -\sigma_{\mathrm{co}}^{-1}\vec{J}^2 \tag{29}$$

Compared with Eqs (27)-(28), the term related to the Seebeck coefficient is absent. In the regions of ceramic plates, energy conservation is defined as:

$$\lambda_{\mathrm{ce}}\frac{d^2T}{dx^2} = 0 \tag{30}$$

In addition to the energy conservation equations of the thermal field, the thermoelectric legs and copper electrodes also follow the conservation equations of the electric field. The current density vector in Eqs (27)-(29) is defined as:

$$\vec{J} = \sigma \vec{E} \tag{31}$$

with

$$\vec{E} = -\frac{d\phi}{dx} + \alpha_{\mathrm{p/n}}(T)\frac{dT}{dx} \tag{32}$$

where, $\vec{E}$ is the electric field density vector, and ϕ is the electric potential.

Also, the electric current through thermoelectric legs and copper electrodes is continuous, which is defined by:

$$\frac{d\vec{J}}{dx} = 0 \tag{33}$$

Eqs (27)-(33) constitute the partial differential equations of the one-dimensional numerical model of TEG. Combined with the thermal field boundary conditions and the electric field boundary conditions, the equations can be solved via numerical methods, such as applying high temperature and low temperature respectively at the hot end and cold end of TEG; setting the sides of TEG exposed to the external environment as heat insulation; setting one terminal of TEG as grounding and another as an input current. The authors in Ref. [41] solved the above equations by using the MATLAB integrated development environment and performed the geometric optimization of the TEG unit. However, in the one-dimensional numerical model, the TEG unit needs to be simplified to a one-dimensional geometry structure, which will lead to an inevitable error. Due to the complexity of the three-dimensional structure of the TEG module, the one-dimensional model can not be used to predict its performance, and it is necessary to extend the numerical model from one dimension to three dimensions.

2.3.2 Three-dimensional steady-state numerical model

The three-dimensional numerical model is more accurate than the one-dimensional numerical model [43] because the directions of electric current and heat flux are not parallel in TEG units and TEG modules. In practical application, an energy recovery circuit is connected with TEG modules to recover the generated electricity. Therefore, the impedance matching characteristics should be considered when studying the output performance of TEG. The transport equations of the three-dimensional steady-state numerical model are consistent with those of the one-dimensional numerical model. For p/n-type thermoelectric legs, the energy conservation is defined as:

$$\nabla \cdot \left(\lambda_{\mathrm{p}}(T)\nabla T\right) = -\sigma_{\mathrm{p}}^{-1}(T)\vec{J}^2 + T\vec{J}\cdot\nabla\alpha_{\mathrm{p}}(T) + \frac{\partial\alpha_{\mathrm{p}}(T)}{\partial T}T\vec{J}\cdot\nabla T \tag{34}$$

$$\nabla \cdot \left(\lambda_{\mathrm{n}}(T)\nabla T\right) = -\sigma_{\mathrm{n}}^{-1}(T)\vec{J}^2 + T\vec{J}\cdot\nabla\alpha_{\mathrm{n}}(T) + \frac{\partial\alpha_{\mathrm{n}}(T)}{\partial T}T\vec{J}\cdot\nabla T \tag{35}$$

With the consideration of impedance matching, the energy conservation of load resistance should also be included in the numerical model, and it is the same as that of copper electrodes, that is:

$$\nabla\cdot\left(\lambda_{\mathrm{m}}\nabla T\right)=-\sigma_{\mathrm{m}}^{-1}\vec{J}^{2} \tag{36}$$

where, the subscript m represents the material regions involved in Fourier heat conduction and electric current flow, co for the copper electrodes, lo for the load resistance, respectively.

For the electrically insulated ceramic plates, Eq. (30) can be extended to Eq. (37), as follows:

$$\nabla\cdot\left(\lambda_{\mathrm{ce}}\nabla T\right)=0 \tag{37}$$

Similarly, the electric field transport equation of the three-dimensional numerical model of TEG includes:

$$\vec{J}=\sigma\vec{E} \tag{38}$$

$$\vec{E}=-\nabla\phi+\alpha_{\mathrm{p/n}}\left(T\right)\nabla T \tag{39}$$

$$\nabla\cdot\vec{J}=0 \tag{40}$$

Besides, the thermal field boundary conditions of the three-dimensional numerical model consist of the first type boundary condition (temperature boundary), the second type boundary condition (heat flux boundary), and the third type boundary condition (convective heat transfer boundary, as defined by Eq. (41)). In most researches [44, 45], the first type boundary condition is applied on both ends of TEG, and the third type boundary condition is applied on the surfaces of TEG exposed to the external environment.

$$-\lambda\frac{\partial T}{\partial n}=h_{\mathrm{ext}}\left(T-T_{\mathrm{ext}}\right) \tag{41}$$

where, h_{ext} and T_{ext} represent the external convective heat transfer coefficient and external temperature, respectively.

There are two kinds of electric field boundary conditions: load resistance boundary condition and the electric current boundary condition. When considering the topological connection of load resistance, one side of the terminals of TEG and load resistance is set to be grounded (U = 0 V), and another side is set to be connected to each other. When replacing the load resistance with an input current, the geometry of load resistance is absent, and one terminal of the TEG is set as the input current boundary, while another terminal is set to be grounded. The direction of the input current is the same as the moving direction of holes in p-type thermoelectric legs, but opposite to the moving direction of electrons in n-type thermoelectric legs. Fig. 5 shows the comparison of numerical results between these two kinds of electric field boundary conditions. Here, the TEG device in Ref. [37] was chosen for the numerical simulation, and other boundary conditions were set as T_h = 450 K, T_c = 310 K, and h_{ext} = 10 W/(m·K). Under the load resistance boundary condition, the load resistance changes from 0.5 Ω to 10 Ω at a rate of 0.5 Ω, while under the electric current boundary condition, the input current changes from 0.1 A to 1.6 A at a rate of 0.1 A. The results indicated that both output voltage and output power predicted by using load resistance boundary conditions are consistent with those predicted by using electric current boundary conditions. Therefore, both can be used to conduct the numerical simulation of TEG devices.

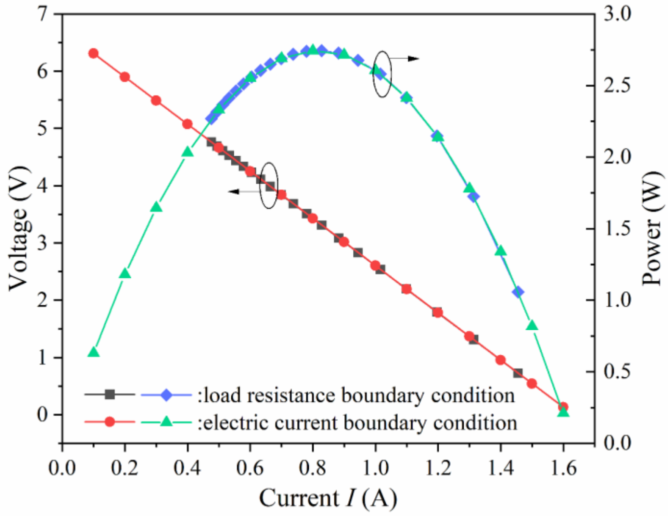

Fig. 5. Comparison of numerical results between load resistance boundary condition and electric current boundary condition.

Chen et al. [46] established a three-dimensional numerical model of the TEG unit by using the user-defined function (UDF) of Fluent, and the model was solved by the FVM computational fluid dynamics (CFD) software package. In their research, the load resistance was incorporated into the input current boundary to handle the field-electric interface, and the distribution characteristics of temperature, Seebeck potential, and heat flux of TEG were successfully obtained, which provides a new modeling approach for predicting the performance of TEG devices. The authors in Ref. [47] investigated the effects of variable material properties and convective heat losses on the performance of the TEG unit using the three-dimensional numerical model. The results indicated that the assumption of constant material properties will underestimate the internal resistance, and the heat loss will slightly enlarge the output power, but significantly lower the conversion efficiency. Based on the three-dimensional numerical model, a multi-objective genetic algorithm was proposed to optimize the geometric structure of TEG element, and the optimal structural design of TEG unit under the first and second type thermal field boundary conditions was studied by Chen et al. [48]. They reported that a smaller leg height enables greater output power under a fixed temperature difference, whereas a larger leg height enables greater output power and conversion efficiency based on a fixed heat flux on the hot end. Fan and Gao [49] proposed a segmented annular TEG unit and utilized the three-dimensional numerical model to analyze its performance. The output power of the segmented annular TEG unit was 18.3% higher than that of the single-Skutterudite annular TEG unit. As can be seen, the three-dimensional numerical model has been widely used to study and optimize the performance of TEG devices because of its high precision.

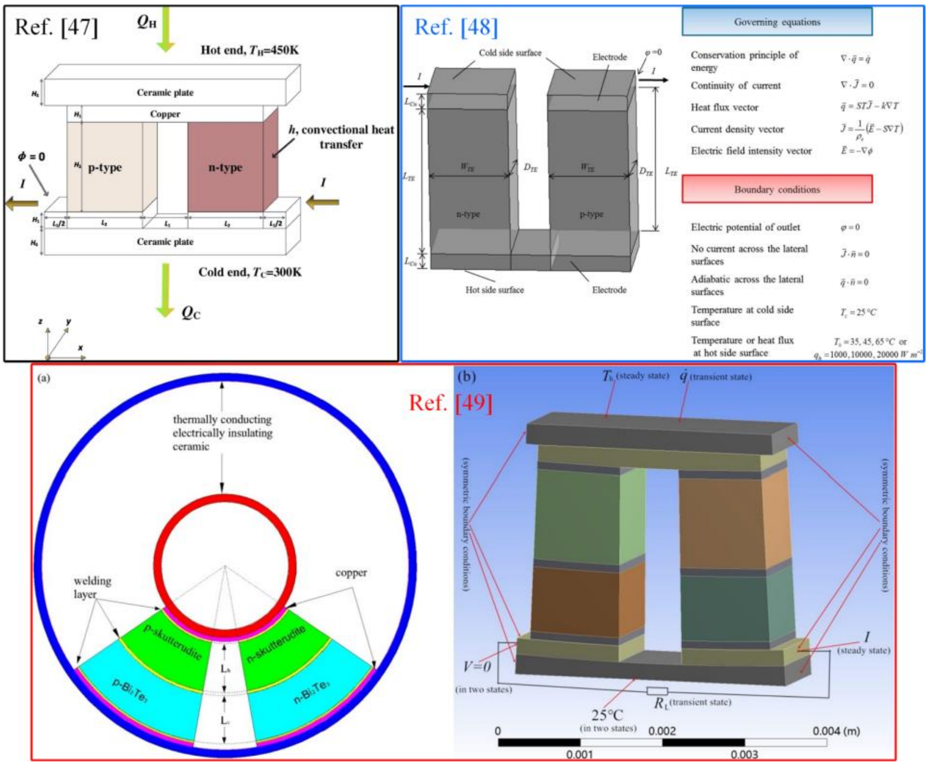

Fig. 6. Schematic of the three-dimensional numerical model and boundary conditions of TEG unit in Refs [47-49].

In the above research [46-49], the electric current boundary condition is used to replace the load resistance to form the circuit loop. Fig. 6 shows the details of the three-dimensional numerical model and boundary conditions in Refs [47-49], in which the numerical simulation is carried out by ANSYS. In practice, TEG is usually connected to an energy recovery circuit, and the electric current is generated naturally under the effect of the temperature difference and thermoelectric coupling effect, therefore, no input current is required, and the load resistance boundary condition is closer to the practical situation than the electric current boundary condition. Besides, the electric field distribution characteristics of load resistance can directly reflect the output performance of TEG. Taking the asymmetric TEG device as the research objective, Luo et al. [50] established a three-dimensional numerical model of the TEG unit considering the topological connection of load resistance, and investigated the influence of the cross-sectional area ratio of the p-type leg and n-type leg on TEG performance. The schematic diagram and numerical results of the TEG unit were shown in Fig. 7, in which the load resistance was electrically connected with the TEG unit, and the numerical simulation was completed by using ANSYS/Thermal-Electric package. According to the numerical results, the optimal cross-sectional area ratio of p-type leg and n-type leg mainly depends on the asymmetric thermoelectric material properties.

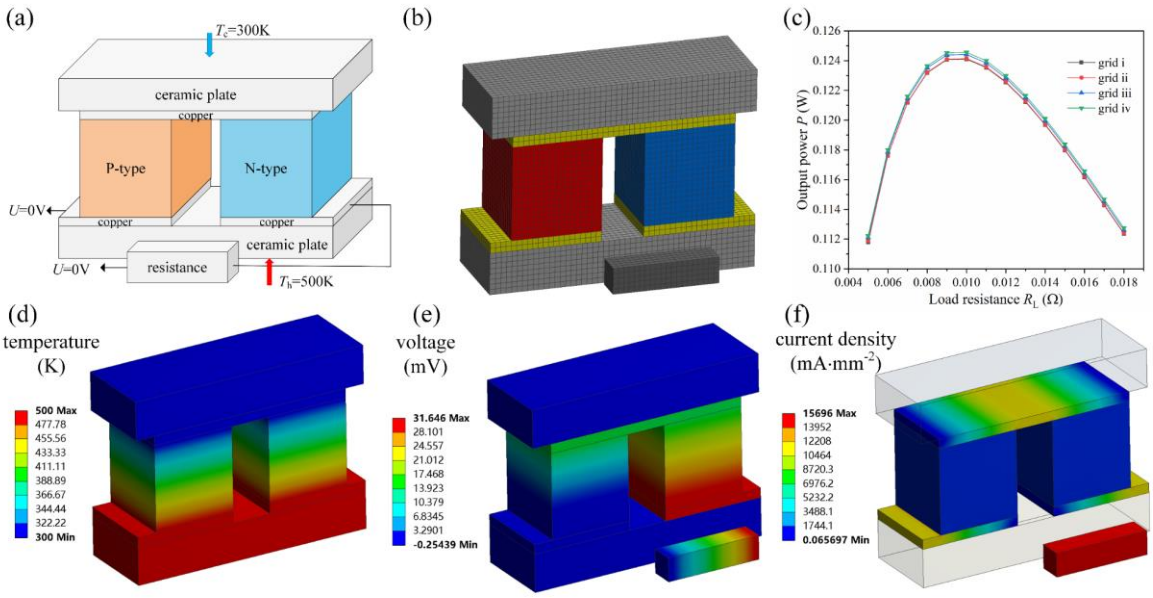

Fig. 7. Schematic of the TEG unit and its numerical results at T_h = 500 K, T_c = 300 K, and h_{ext} = 0 [50]. (a) Boundary conditions. (b) Three-dimensional finite element model. (c) Grid independence examination. (d) Temperature distributions. (e) Voltage distributions. (f) Current density distributions.

Furthermore, the three-dimensional numerical model can be extended from the TEG unit to the TEG module by establishing the three-dimensional CAD geometry of the TEG module and considering the topological relationship among TEG units. Based on simulation platforms of ANSYS and ANSYS/Thermal-Electric respectively, Ming et al. [51] and Luo et al. [37] have carried out numerical simulations on the TEG module and studied the influence of structural parameters on the performance of the TEG module. Also, COMSOL Multiphysics is a powerful tool to simulate the multiphysics coupling phenomena, and more and more researchers use it to predict the performance of TEG devices [52]. Hu et al. [53] used COMSOL to calculate the three-dimensional numerical model and predict the behavior of a nanostructured PbTe-based TEG module, as shown in Fig. 8. In the study, only the grounding boundary condition needs to be defined to compute the electric field governing equations, and the load resistance was set to be in electrical and thermal contact with TEG module. Through finite element simulations, the physical field distribution characteristics of the whole geometry were obtained, including temperature, voltage, heat flux, Joule heat, and *ZT* values. Compared with the ANSYS/Thermal-Electric simulation platform [37, 50], the load resistance in COMSOL follows the governing equations of Eqs (36) and (38)-(40), while in ANSYS/Thermal-Electric, the load resistance only involves the calculation of electric field governing equations of Eqs (38)-(40). The difference in numerical results between these two solvers can be ignored because the Fourier heat conduction of load resistance has an insignificant influence on the temperature distributions of the whole TEG module [54].

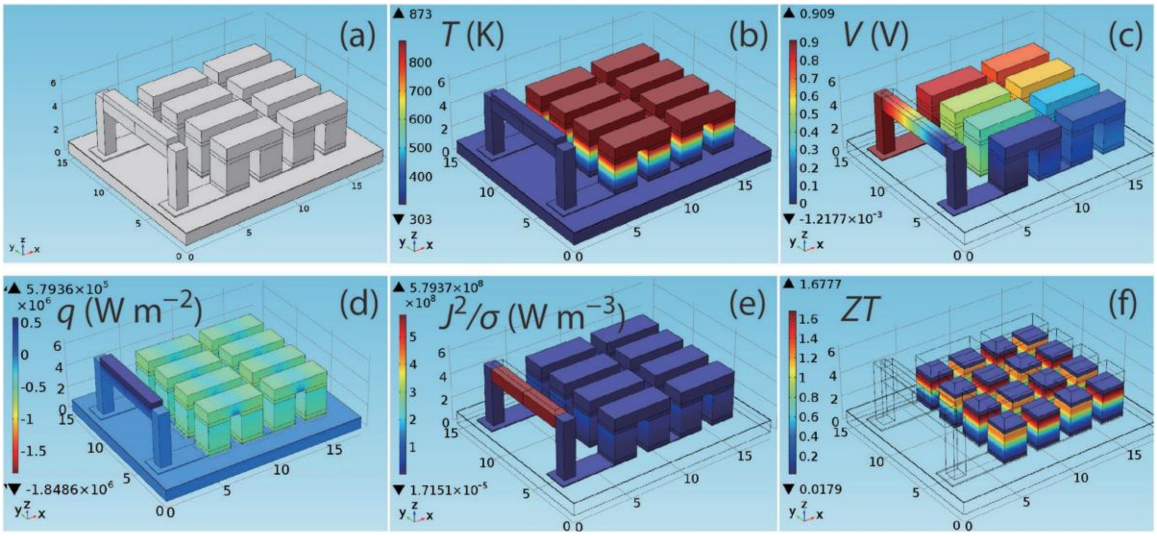

Fig. 8. Numerical results of a TEG module predicted by COMSOL Multiphysics [53]. (a) Three-dimensional geometry. (b) Temperature distributions. (c) Voltage distributions. (d) Heat flux distributions. (e) Joule heat density distributions. (f) *ZT* values of thermoelectric materials.

2.3.3 Transient numerical model

Compared with the thermal resistance model, the numerical model can not only predict more reasonable results but also can be used to predict the transient performance of TEG. In some applications, the heat source is time-dependent, for example, the automotive exhaust temperature changes with the vehicle speed; the flame temperature of the stove-powered TEG system is not static; the TEG will show dynamic characteristics during the start-up or shut-down stages. Consequently, it is necessary to build a transient numerical model to predict the dynamic response characteristics of TEG devices. In order to extend the numerical model from a steady state to a transient state, the term concerning the transient internal energy change should be included in the energy conservation equations. The thermal field transport equations of the transient numerical model are as follows:

$$(\rho c)_{\mathrm{p}} \frac{\partial T}{\partial t} = \nabla \cdot \left(\lambda_{\mathrm{p}}(T) \nabla T\right) + \sigma_{\mathrm{p}}^{-1}(T) \vec{J}^{2} - T\vec{J} \cdot \nabla \alpha_{\mathrm{p}}(T) - \frac{\partial \alpha_{\mathrm{p}}(T)}{\partial T} T\vec{J} \cdot \nabla T \tag{42}$$

$$\left(\rho c\right)_{\mathrm{n}}\frac{\partial T}{\partial t}=\nabla\cdot\left(\lambda_{\mathrm{n}}\left(T\right)\nabla T\right)+\sigma_{\mathrm{n}}^{-1}\left(T\right)\vec{J}^{2}-T\vec{J}\cdot\nabla\alpha_{\mathrm{n}}\left(T\right)-\frac{\partial\alpha_{\mathrm{n}}\left(T\right)}{\partial T}T\vec{J}\cdot\nabla T \tag{43}$$

$$\left(\rho c\right)_{\mathrm{m}}\frac{\partial T}{\partial t}=\nabla\cdot\left(\lambda_{\mathrm{m}}\nabla T\right)+\sigma_{\mathrm{m}}^{-1}\vec{J}^{2} \tag{44}$$

$$\left(\rho c\right)_{\mathrm{ce}}\frac{\partial T}{\partial t}=\nabla\cdot\left(\lambda_{\mathrm{ce}}\nabla T\right) \tag{45}$$

where, ρ is the density, c is the specific heat, and t is the time. Other symbols and subscripts have the same meaning as those of the steady-state numerical model. The term on the left hand of Eqs (42)-(45) represents the transient internal energy change.

As for the electric field, the governing equations of the transient numerical model are the same as Eqs (38)-(40) in the steady-state numerical model, and the only difference is that all variables in the transient numerical model are time-dependent.

Combined with the transient boundary conditions, the transport equations (Eqs (38)-(40) and (42)-(45)) of the transient numerical model can be worked out by using numerical analysis tools. Transient boundary conditions generally refer to the transient input of heat source, including the first type transient boundary condition of temperature $T_{\mathrm{h}}(t)$ and the second type transient boundary condition of heat flux $\dot{q}(t)$. The cold side thermal field boundary conditions and ambient convection heat transfer boundary conditions can be set as steady state or transient state according to actual situations. However, the boundary conditions of the electric field are all steady state, because the dynamic electric field parameters respond correspondingly with the transient change of temperature.

Yan and Malen [55] simplified the transient numerical model from three-dimensional to one-dimensional, and solved the one-dimensional transient numerical model by a central difference approximation and explicit time matching method. When applying a periodic heat flux on the hot end and adopting the current boundary condition to replace the load resistance, the numerical results indicated that the periodic heat source can amplify the heat-to-electric conversion efficiency of TEG. Based on the previous steady-state works, Meng et al. [56] further proposed a transient numerical model of the TEG unit to deeply investigate its dynamic response characteristics under transient boundary conditions (including variations of hot side temperature, cold side temperature, and load current). Some useful results were obtained by their research, such as the response hysteresis of output power was founded due to the delay of thermal diffusion, as shown in Fig .9. However, the research on the temperature-dependent properties of thermoelectric materials and geometric dimensions of TEG unit is still insufficient in their study. For this reason, Jia et al. [57] developed a two-dimensional transient numerical model considering the temperature-dependent thermoelectric material properties, and utilized the model to investigate the transient behavior of a linear-shaped TEG unit under different thermal load and geometric dimensions of legs. The numerical simulation was carried out by ANSYS, and the results contributed to further understanding the transient behavior of TEG. But the transient numerical model used by the authors is two-dimensional.

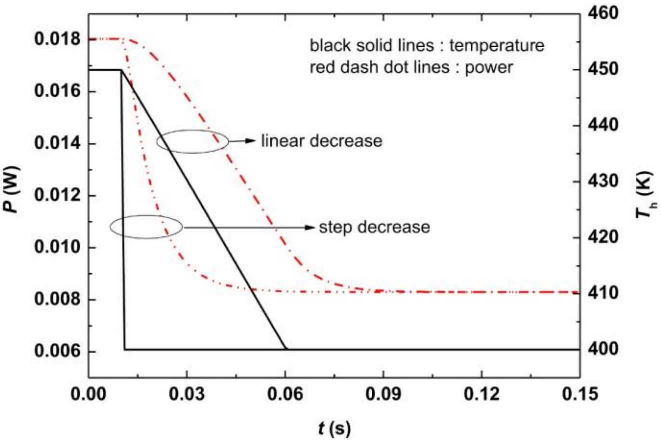

Fig. 9. Dynamic output power variations under step and linear decrease in hot side temperature [56].

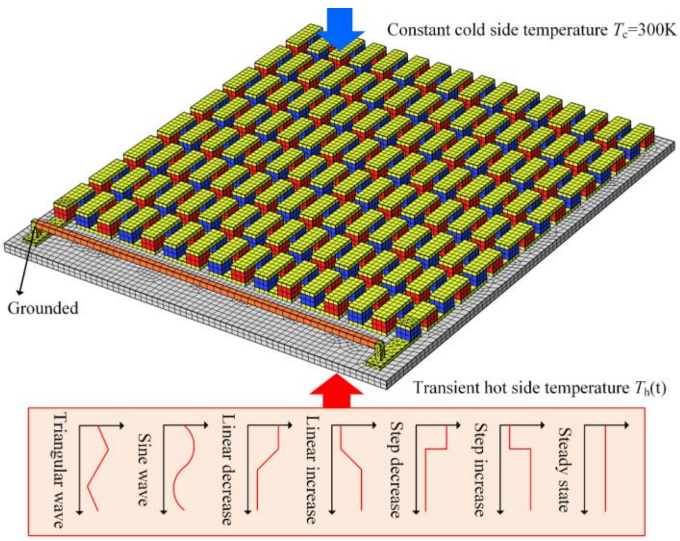

Fig. 10. Finite element features and boundary conditions of the transient numerical model of TEG module [58].

To be more accurate, a complete three-dimensional transient numerical model considering the temperature-dependent properties and the topological connection of load resistance was proposed by Luo et al. [58]. Also, the authors extended the transient numerical model from a TEG unit to a TEG module, and the finite element simulations were conducted via COMSOL. Fig. 10 shows the finite element features and boundary conditions of the transient numerical model of the TEG module. By comparing the numerical results under different transient temperature excitations, they reported that the time delay of the output response of the TEG module is contingent on the rate of temperature change, the dynamic response characteristic of conversion efficiency is synchronous with that of output power, and the periodic temperature excitation may amplify the output power, but does not affect the conversion efficiency. The findings are helpful to deeply understanding the dynamic response characteristics and the causes, and the developed transient numerical model of the TEG module can be further extended to the whole TEG system.

2.4 Analogy models

Based on the analogy between thermal and electrical variables, the thermal resistance model can be equivalent to an electrical circuit model [59]. In an electrothermal analogy, heat flow is expressed as current, the temperature is expressed as voltage, and thermal resistance is expressed as electrical resistance. The heat and cooling source can be represented as the ideal voltage source, and the zero temperature is the electrical ground. The supplemented current sources can represent the internal heat sources like Peltier heat, Joule heat, and so on [60]. Through the electrothermal analogy, the thermal resistance model mentioned in Section 2.2 can be worked out by an equivalent circuit. On the platform of the SPICE simulation program, the equivalent circuit model considering the temperature dependence of material properties was established by Mitrani et al. [61], in which the equivalent electrical circuit represented by thermal variables is connected with a pure load circuit. The model results were in good agreement with those predicted by a one-dimensional numerical model.

In addition, the equivalent electrical circuit model facilitates the transient simulation by applying transient temperature (voltage) inputs on both ends (two terminals of the equivalent circuit) of TEG. The one-dimensional transient differential governing equation of thermoelectric legs is [60]:

$$\begin{aligned} dQ_{\mathrm{p/n}} &= Q_{\mathrm{p/n}}\left(x+dx\right)-Q_{\mathrm{p/n}}\left(x\right) \\ &= c_{\mathrm{p/n}} m_{\mathrm{p/n}} \frac{dT_{\mathrm{p/n}}\left(x\right)}{dt} + I^2 \frac{\sigma_{\mathrm{p/n}}^{-1}\left(T_{\mathrm{p/n}}\left(x\right)\right)}{A_{\mathrm{p/n}}} dx + d\alpha_{\mathrm{p/n}}\left(T_{\mathrm{p/n}}\left(x\right)\right) T_{\mathrm{p/n}}\left(x\right) I \end{aligned} \tag{46}$$

where, $c_{\mathrm{p/n}}$ and $m_{\mathrm{p/n}}$ are respectively the specific heat and mass of p-type and n-type legs. The first term is the transient term, which can be represented by paralleling an electrical capacitor C_{e} in the equivalent circuit. Also, the transient heat transfer term can be modeled by an electrical analogy of a capacitor, which is:

$$I_{\mathrm{e}} = C_{\mathrm{e}} \frac{dV_{\mathrm{e}}}{dt} \tag{47}$$

where, C_{e} is taken as $c_{\mathrm{p/n}} m_{\mathrm{p/n}}$, and V_{e} is the equivalent voltage of temperature $T_{\mathrm{p/n}}(x)$. Consequently, the transient term can be considered as an analogy of supplemented current source I_{e}.

An accurate TEG analogy model was proposed and implemented in a SPICE environment by Chen et al. [60], as shown in Fig. 11. The model took into account all temperature-dependent characteristics of thermoelectric materials and all heat source terms, and it was validated with one-dimensional numerical simulation results from ANSYS and experimental data from an actual TEG module, respectively. Their research provides useful guidance for the electrothermal modeling of TEG devices. However, the thermal resistances from ceramic plates to thermoelectric legs are omitted, and the heat source temperature and cooling source temperature of the TEG module are directly used as the working temperatures of legs in their study. Fisac et al. [62] proposed an improved analogy model considering the thermal resistances from ceramic plates to legs, as shown in Fig. 12. The model was used to study the transient response characteristics of the TEG module under conditions of smaller thermal inertia, and the results indicated that the response time of TEG module depends on the structural characteristics.

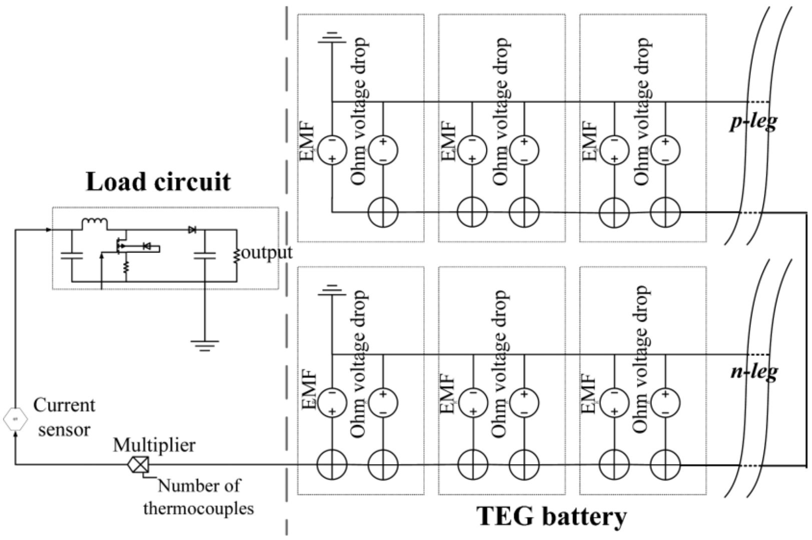

Fig. 11. Equivalent circuit of the thermoelectric battery model [60].

The analogy model is derived from the equations of the thermal resistance model, therefore, it can only deal with a one-dimensional thermoelectric phenomenon, and can not consider the ambient convection heat loss. In previous research [63, 64], the software of SPICE was commonly used to establish and solve the equivalent circuit model. Compared with the thermal resistance model, the analogy model has advantages in predicting the dynamic performance of the TEG module, because the transient heat transfer term can be represented as a supplementary current source in the equivalent circuit. The transient characteristics of the TEG module can be obtained under the condition of pulse input. The analogy model also facilitates the simulation of a TEG module and its interconnections with electronic control circuits, such as the maximum power point tracking circuit.

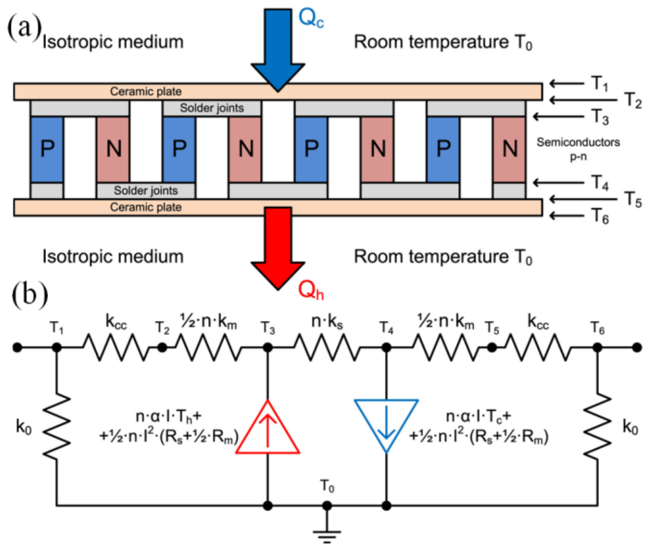

Fig. 12. Schematic diagram of TEG module with different temperatures (a) and the equivalent electrical circuit model (b) [62].

2.5 Comparison of different models

In recent years, great progress has been made in the theoretical models of TEG devices. From TEG unit to TEG module, from one-dimensional to three-dimensional, from steady-state to transient state, more and more complete theoretical models have been proposed by researchers. In general, theoretical models can be classified into three categories: thermal resistance model, numerical model, and analogy model. Taking a thermoelectric element as the research objective, Fraisse et al. [22] compared the prediction results of one-dimensional models, including the thermal resistance model, analogy model, and numerical model. The numerical simulation was performed by the finite element method of ANSYS. According to their research, the results predicted by the numerical model are consistent with those predicted by the analogy model, but the thermal resistance model may overestimate the output voltage and power. By comparing the simplified thermal resistance model with the three-dimensional numerical model, the same conclusions were obtained by Meng et al [47].

In summary, the numerical model can take into account various factors in the actual situation, such as the temperature dependence of thermoelectric materials, three-dimensional geometry, transient response characteristics, and so on, which is the most reasonable theoretical model. But the numerical model suffers from a relatively long computation time. The thermal resistance model has the advantages of short calculation time and no complicated modeling process, but the model error is larger than the numerical model. The analogy model can be used to study the dynamic response characteristics of TEG devices under pulse input, also, it facilitates the joint simulation with electronic control circuits. However, the analogy model is derived from the basic equations of the thermal resistance model, rendering inevitable errors. Due to the advantages of the high accuracy and the visualization of physical field distribution characteristics, the numerical model has become the most commonly used model to predict the performance of TEG devices.

In Table 1, recent works on the theoretical model of TEG devices are presented. As can be seen, the development of theoretical models for predicting the performance of TEG devices has been mature. In practical application, TEG modules are usually placed between the heat collector and the radiator as the power supply. However, the working temperature of TEG modules is unknown and difficult to be measured directly, which leads to the theoretical models of TEG devices being unable to be solved. The data that can be measured directly include the parameter characteristics of the heat source or cooling source. Therefore, it is necessary to establish some comprehensive models of the TEG system to predict its performance, taking into account the heat transfer process from heat/cooling sources to hot/cold sides of TEG modules.

Table 1. Summary of theoretical models of TEG devices.

Model	Dimensions	Using simplified temperatures	Considering temperature-dependent properties	Steady/transient state	TEG unit/module	Sources
Thermal resistance model	1-D	yes	no	steady state	TEG unit	[22, 30, 47]
		yes	no		TEG module	[31, 32]
		no	no		TEG unit	[65, 66]
		no	no		TEG module	[34, 35]
		no	yes		TEG unit	[16, 33]
		no	yes		TEG module	[25]
Numerical model	1-D	no	yes	steady state	TEG unit	[22, 40-42]
	3-D		no	steady state	TEG unit	[21, 43, 49]
	3-D		no	steady state	TEG module	[21, 67]
	3-D		yes	steady state	TEG unit	[36, 38, 44-48, 50]
	3-D		yes	steady state	TEG module	[37, 39, 51-53, 68, 69]
	1-D		no	transient state	TEG unit	[55]
	3-D		no	transient state	TEG unit	[56]
	2-D		yes	transient state	TEG unit	[57]
	3-D		yes	transient state	TEG module	[58]
Analogy model	1-D	no	yes	steady state	TEG unit	[22]
		no	yes	steady state	TEG module	[61]
		yes	no	transient state	TEG module	[70]
		yes	yes	transient state	TEG module	[60]
		no	no	transient state	TEG module	[62]
		no	yes	transient state	TEG module	[63, 64]

3. Theoretical models of thermoelectric generator systems

Due to the advantages of no moving parts, no pollution, and long service life, a large number of TEG systems have been developed to harvest thermal energy and generate electricity. The condition where the TEG module is used and the nature of the heat source are two classification criteria for TEG systems [71]. According to the condition where the TEG is used, TEG systems can be grouped into six categories:

i) radioisotope TEG systems: the natural radioactive decay energy of radioactive elements is used as the heat source to produce electricity for electronics, such as power supply in the field of space exploration;

ii) solar-based TEG systems: the solar energy is used as a heat source;

iii) stove-powered TEG systems: the source of energy is from burning solid fuels, such as power supply in the field of combined heat and power generation system;

iv) wearable TEG systems: the source of energy comes from the heat of the human body;

v) micro-generation for sensors and microelectronics: the power level is very low and all sources of heat are feasible;

vi) waste heat recovery: the TEG system is used to recover the waste heat contained in thermal fluids, such as exhaust waste heat from automobiles, aircraft and helicopters, ships, and industries.

To predict the performance of the above TEG systems, several theoretical models for the corresponding TEG systems are proposed, such as FEM/FVM-based numerical models and thermal resistance-based analytical models. According to the different physical fields involved, the FEM/FVM-based numerical models are classified into three groups: thermal-electric numerical models, fluid-thermal numerical models, and fluid-thermal-electric numerical models. The performance of different TEG systems can be estimated by the same theoretical model, for example, the thermal-electric numerical model can predict the output performance of radioisotope, solar-based, stove-powered, and wearable TEG systems by setting different boundary conditions. Consequently, the condition where the TEG is used can not be used as the classification criteria for the theoretical models of the TEG system. Based on the nature of the heat source, the theoretical models of the TEG system are grouped into two categories in this chapter: TEG systems directly contacted with the heat source and TEG systems for fluid waste heat recovery.

3.1 Thermoelectric generator systems directly contacted with the heat source

In radioisotope, solar-based, stove-powered, and wearable TEG systems, the heat source is directly in contact with TEG modules or indirectly through a heat transfer unit. The thermal resistance model in section 2.2 and the numerical model in section 2.3 can be used to predict their performance under different heat sources. When a heat transfer unit is placed between the heat source and the TEG module, the output performance of the TEG module can be estimated by adding parasitic thermal resistances to the thermal resistance model or adding an energy conservation differential equation to the numerical model. For the heat dissipation of TEG systems, there are two cooling modes: natural air cooling and water cooling, which can be characterized by the convective heat transfer analysis.

3.1.1 Thermal resistance-based analytical model

Using solar energy as a heat source, He et al. [72] reported a solar heat pipe TEG system comprising a TEG module, a finned heat pipe, and an evacuated double-skin glass tube. The system takes advantage of the heat pipe to convert the solar irradiation into a heat flux to meet the TEG working requirement. Also, water cooling is adopted in the system. The authors integrated Eqs (48)-(49) into the simplified thermal resistance model to calculate the output power and conversion efficiency of the system, and then studied the influence of solar irradiation, cooling water temperature, thermoelectric leg length and cross-sectional area, and the number of TEG units, etc. on the maximum power output and conversion efficiency of the TEG system. Some optimal structural parameters were obtained. In the subsequent work [73], the authors improved the model by considering the contact thermal resistance and conductive thermal resistance from the heat pipe and radiator to the hot and cold side of thermoelectric legs respectively. According to the improved model, the Peltier cooling and heating performance of the thermoelectric module was investigated. However, the thermoelectric material properties used in the model are constant. The accuracy of the model can be further improved by considering the temperature dependence of thermoelectric materials.

$$Q_{\mathrm{h}} = h_{\mathrm{hp}} A_{\mathrm{hp}} \left(T_{\mathrm{hp}} - T_{\mathrm{h}} \right) = \alpha_{\mathrm{pn}} I T_{\mathrm{h}} + \frac{T_{\mathrm{h}} - T_{\mathrm{c}}}{R_{\mathrm{leg}}} - \frac{1}{2} I^2 R_{\mathrm{in}} \tag{48}$$

$$Q_{\mathrm{c}} = h_{\mathrm{wa}} A_{\mathrm{ce}} \left(T_{\mathrm{c}} - T_{\mathrm{wa}} \right) = \alpha_{\mathrm{pn}} I T_{\mathrm{c}} + \frac{T_{\mathrm{h}} - T_{\mathrm{c}}}{R_{\mathrm{leg}}} + \frac{1}{2} I^2 R_{\mathrm{in}} \tag{49}$$

where, h_{hp} is the heat transfer coefficient between the heat pipe condenser and the ceramic plate of the TEG module, A_{hp} is the plate copper fin area, T_{hp} is the temperature of the heat pipe, h_{wa} is the effective heat transfer coefficient between the cooling water and the ceramic plate, A_{ce} is the area of ceramic plate, and T_{wa} is the temperature of cooling water.

Stove-powered TEG systems show great potential in developing countries, which can not only improve the air-fuel ratio by using an electric fan to realize complete combustion in the stoves but also meet the power supply requirements of low-power electronic products such as lights and phones [74]. The thermal resistance model is the most commonly used method to predict the performance of stove-powered TEG systems. Similarly, Champier et al. [74] established a theoretical model by integrating the thermal resistance between the heat (cooling) source and TEG module into the simplified thermal resistance model in section 2.2.1. In their research, the average temperature $T_a = (T_h + T_c)/2$ was used to evaluate the thermoelectric material properties, and the temperature of the heat source and cooling source was measured by thermocouples. According to the temperature data at different time points, the output power of a stove-powered TEG system developed by the authors was analyzed and verified by experimental results. Considering the heat radiation of the hot source and cooling source, Najjar and Kseibi [75] carried out a comprehensive heat transfer and performance analysis of a multi-purpose stove-powered TEG system. The modeling process for all the subcomponents was described in detail, and the research results provided powerful guidance for further improving the thermal resistance-based analytical model of stove-powered TEG systems.

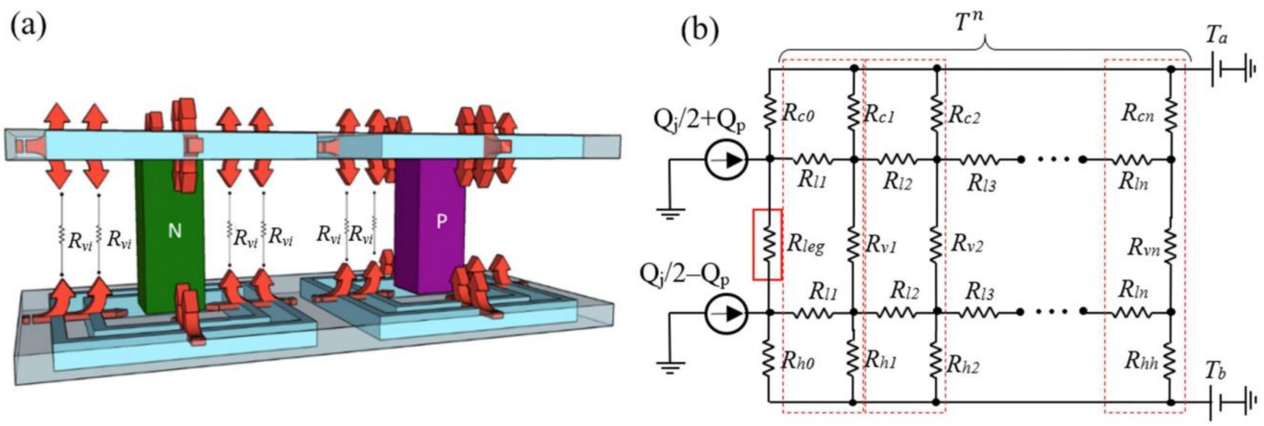

Fig. 13. Schematic of the quasi three-dimensional thermal resistance model of wearable TEG module [76].

Wearable TEG systems can continuously convert body heat into electrical energy, attracting lots of interest in self-powered electronic devices. The performance of wearable TEG systems is limited by the large external thermal resistances, and it is desirable to design a TEG module with a substantially larger thermal resistance than the external thermal resistances. It seems that the thermoelectric leg should be designed with a high height-to-area ratio. However, due to body comfort and the increase in internal resistance, the leg height can not be increased indefinitely. Therefore, the parameters of TEG legs should be balanced between performance and wearability. Nozariasbmarz et al. [76, 77] proposed a quasi three-dimensional thermal resistance model to optimize the parameters of the TEG module, as shown in Fig. 13. In the model, according to the distance between the thermoelectric leg and the leg center, thermoelectric legs were divided into different rectangular rings and characterized by different thermal resistances. In addition, the contact thermal resistance from the skin to TEG module, and the convective thermal resistance from the heat sink to ambient were taken into account. Based on the developed model, the structural parameters of the wearable TEG system were optimized.

In the modeling of the radioisotope TEG system, few papers are using the thermal resistance model to predict its performance, because the heat transfer from the radioisotope heat source to the hot side of the TEG module can not be represented as thermal resistance. More importantly, the TEG modules used in the system usually present a radial shape instead of the conventional π shape. The research objective of the thermal resistance model is based on the TEG module with a π shape. Therefore, researchers prefer to use a numerical model to predict the performance of radioisotope TEG systems, because the numerical model is not limited to geometric shapes of TEG modules.

When using thermal resistance-based analytical models to predict the performance of solar-based, stove-powered, and wearable TEG systems, it is recommended to consider the thermal resistance of all components, including convective thermal resistance, contact thermal resistance, and conductive thermal resistance. Besides, due to the high dependence of thermoelectric materials on temperature, the assumption of constant Seebeck coefficient, thermal conductivity, and electric resistivity has a great influence on the model accuracy. On the other hand, it is not accurate enough to use the average temperature to evaluate the properties of thermoelectric materials due to the nonlinearity of thermoelectric material properties. Therefore, appropriate methods should be adopted to deal with the temperature dependence of the thermal resistance model, such as the iterative calculation method described in Fig. 4. For the transient performance analysis of these TEG systems, the thermal resistance-based analytical model suffers from the same problems as the thermal resistance model of TEG module, as mentioned in the last paragraph of Section 2.2.

3.1.2 Thermal-electric numerical model

For TEG systems directly contacted with the heat source, the thermal-electric multiphysics coupled numerical model has been widely used to simulate precisely the thermoelectric conversion process and optimize the geometrical size of TEG systems. The TEG modules contained in the system can be modeled by the transport equations in Section 2.3.2, and the heat transfer components placed on both sides of TEG modules can be characterized by Eq. (37).

In the field of radioisotope TEG system, Liu et al. [78] utilized the thermal-electric numerical model to optimize the structural size of a micro-radial milliwatt-power radioisotope TEG system. A solid heat transfer unit was placed in the center of the system as the equivalent heat source of ^{241}Am isotope element. During the numerical simulation, the solid heat transfer unit provided a constant heat source temperature, which was set to contact with the hot side of the TEG legs, and was set to be grounded in the current unit. Also, the TEG system was exposed to the indoor environment with an air convection coefficient of 6 W/(m^2·K). Ultimately, the temperature distributions and the open-circuit voltage of the

TEG system were obtained by numerical simulations in the platform of COMSOL. Through the optimization, the open-circuit voltage of 605.84 mV and the maximum output power of 423.50 μW were obtained. Khajepour and Rahmani [79] proposed a multi-stage design method for the radioisotope TEG system, in which COMSOL was used for thermal-electric numerical simulation to determine the parameters of the TEG module, and ANSYS was used for thermal numerical simulation to determine the parameters of isotope heat source and its accessories. However, the load response characteristics were ignored in Refs [78, 79]. It is not accurate enough to use the open-circuit voltage to evaluate the output performance of the TEG system, because the load resistance at the maximum output power is higher than the internal resistance of the TEG module, which is different from the common circuit [50].

In the field of solar-based TEG systems, Liu et al. [80] proposed a novel solar TEG module design to enhance the output power and conversion efficiency, which combines the asymmetric legs with the variable cross-sectional area and segmented thermoelectric materials. The geometric parameters of the legs were optimized by the thermal-electric numerical model, and the numerical simulation was carried out by COMSOL software. In the model, a heat flux boundary condition was applied on the hot side of the TEG module, a heat sink with a constant temperature of 300 K was applied on the cold side of the TEG module, and a current input boundary condition was adopted to form a circuit. Here, the heat flux absorbed from solar energy is defined by the following formula [81]:

$$q = q_{\mathrm{solar}} C_{\mathrm{g}} A_{\mathrm{ce}} \eta_{\mathrm{opt}} a_{\mathrm{ce}} \tag{50}$$

where q_{solar} is the solar irradiance. C_{g} is the concentration ratio, which is estimated by the area of the lens divided by that of the collector. A_{ce} is the cross-sectional area of the collector and is usually equal to the cross-sectional area of the ceramic plate. η_{opt} is the optical efficiency of the Fresnel lens. a_{ce} is the absorptivity of the collector coating. Generally, parameters in Eq. (50) are given values in a specific numerical simulation. Thus, the performance of a solar-based TEG system can be predicted under specific solar energy input.

For the application of thermoelectric power generation in the field of self-powered wearable devices, the TEG module usually works under a small temperature gradient, such as the temperature difference between body temperature and ambient temperature. To maintain the wearability and flexibility of devices, Francioso et al. [82] fabricated a flexible heat sink-free wearable TEG system, in which two metal layers were screen-printed on both ends of the TEG module. The hot side metal layer was to enhance the thermal contact with the skin, and the cold side one was to enhance the heat dissipation and lower the thermal resistance of ambient air. As already discussed, the leg height, as well as the height of the metal layer, have opposite effects on the output performance and wearability. For this reason, the thermal-electric numerical model was adopted to determine the optimal ones. Under the boundary conditions of constant heat flux at the hot end and natural convection on the cold end, the numerical simulations were performed by using COMSOL software. The results indicated that the optimal leg heigh and Ag metal layer height are 2 mm and 500 μm respectively. However, the thermoelectric material properties were assumed to be constant in their study. The use of flexible encapsulation is an effective approach to maintain flexibility and protect the TEG legs against mechanical vibration and reduce stress. Based on the thermal-electric numerical model, Liu et al. [83] conducted a comprehensive performance evaluation for a wearable TEG module with flexible encapsulation. In the modeling, the practical boundary conditions have been completely considered, including the temperature-dependent thermoelectric material properties, the natural convection heat transfer, and the topological connection of load resistance. The results showed that the average performance deviation between the model results and the experimental data was 4.2%. Under the fixed temperature difference of 15 K, the maximum output power of the optimized wearable TEG module is 598.1% higher than that of the original design. Some useful results were obtained in their study.

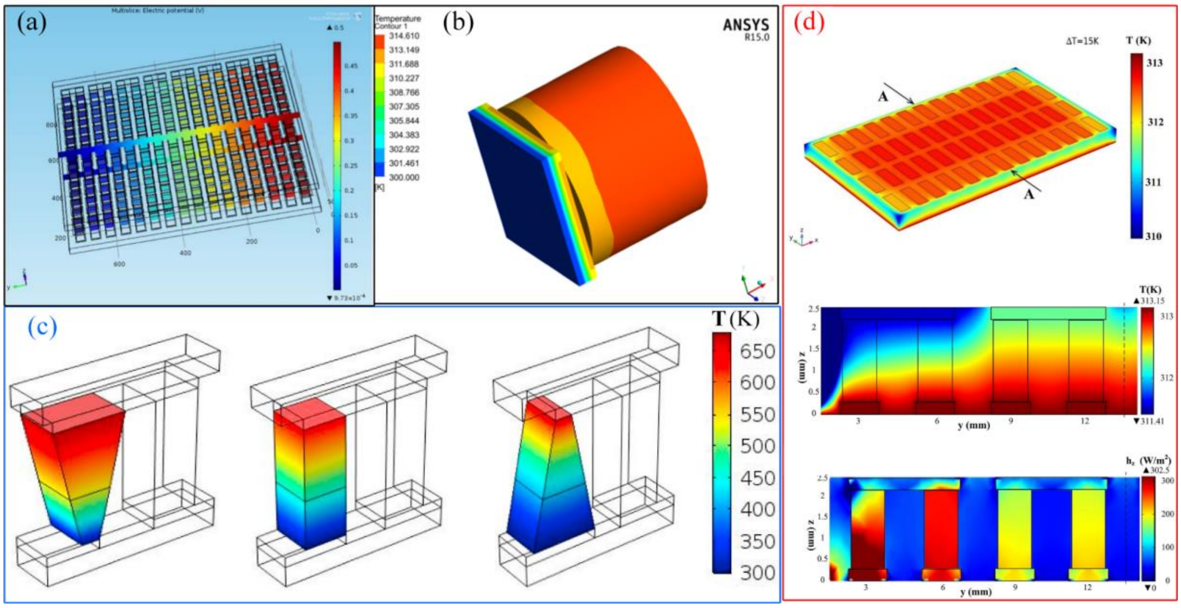

Fig. 14. Numerical results of TEG systems directly contacted with the heat source reproduced from Refs [79, 80, 83]. (a) Open-circuit voltage distribution of a radioisotope TEG module obtained by COMSOL [79]; (b) Temperature distributions of a radioisotope TEG module and its heat source obtained by ANSYS [79]; (c) Temperature profile of a solar-based TEG unit obtained by COMSOL [80]; (d) Temperature and heat flux profiles of a wearable TEG module obtained by COMSOL [83].

It can be seen that numerical modeling plays a significant role in predicting and optimizing the performance of TEG systems. Fig. 14 shows the numerical results of radioisotope, solar-based, and wearable TEG systems in Refs [79, 80, 83], respectively. The thermal-electric numerical model of the TEG module has been widely adopted to study its characteristics in these application scenarios, in which the heat transfer components on both sides of the TEG module were omitted by setting appropriate thermal boundary conditions. Compared with the thermal resistance-based analytical model, the thermal-electric numerical model can consider all the actual boundary conditions and predict more reasonable results. However, there were few reports on numerical modeling of the stove-powered TEG system, and researchers mainly used the thermal resistance-based analytical model to study its performance. Numerical investigation on the stove-powered TEG system may grow up in future works.

Another unparalleled advantage of the numerical model is that it is capable of predicting the transient behavior of TEG systems directly contacted with the heat source. By extending the transient numerical model in Section 2.3.3 from the TEG module to the TEG system and combining it with transient hot side temperature input, the transient performance prediction can be completed by using numerical analysis software (e.g. COMSOL Multiphysics). The transient temperature variation of the heat source can be obtained through experimental measurement. At present, most researches focus on steady-state performance analysis. In practical application, the heat source is not static. It is more meaningful to study the dynamic response characteristics of the TEG system.

3.2 Thermoelectric generator systems for fluid waste heat recovery

In recent decades, thermoelectric power generation technology has aroused great interest in the field of fluid waste heat recovery, such as automobile exhaust waste heat recovery, industrial waste heat recovery, ship exhaust waste heat recovery, and so on, among which the automobile exhaust waste heat recovery is the most popular research object. For automobile engines, about one-third of the heat generated by burning fossil fuels is directly discharged into the environment in the form of exhaust gases, causing serious energy shortage and environmental pollution [84]. Thermoelectric power generation is an effective manner to recover the heat energy from exhaust gases, and the electricity generated by the TEG system can be used for the power supply of vehicle electronics or stored in a battery. A great number of automotive TEG system prototypes have been developed by researchers [85, 86]. The results showed that the maximum output power of the automotive TEG system can reach 500-1000 W, which exhibits a good application prospect.

In order to predict and optimize the performance of automotive TEG systems, several theoretical models have been proposed in previous studies. According to different principles, theoretical models can be grouped into three categories: thermal resistance-based analytical model, computational fluid dynamics (CFD) model, and fluid-thermal-electric multiphysics field coupled numerical model. Compared with TEG systems directly contacted with the heat source, the automotive TEG system involves complex fluid flow, which brings great difficulties to the modeling process. In addition, the theoretical model of the automotive TEG system can be used to predict the characteristics of the TEG system in other fluid waste heat recovery applications, because they follow the same governing equations.

3.2.1 Thermal resistance-based analytical models

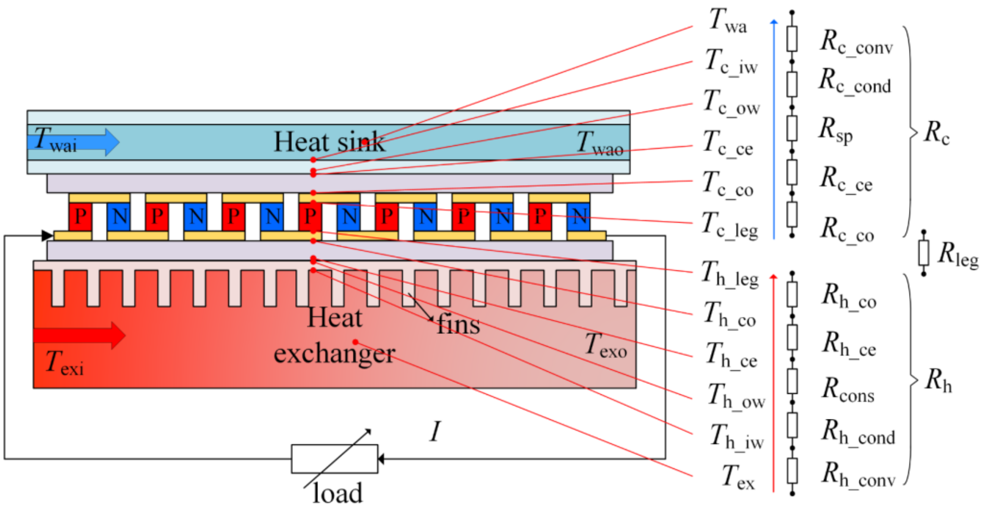

Fig. 15. Schematic diagram of the thermal resistance network of the water-cooled automotive TEG system.

In order to effectively dissipate heat and reduce the cold side working temperature of the TEG module, the water cooling mode is a more attractive method than the air cooling mode. Besides, the heat transfer process of water cooling is more complex than that of air cooling, because air cooling can be estimated by a convective thermal resistance. Therefore, the water-cooled automotive TEG system is taken as the objective to elucidate the thermal resistance-based analytical model in this section. Fig. 15 shows the schematic diagram of the thermal resistance network of the water-cooled automotive TEG system. In most cases, the known parameters of the automotive TEG system only include given temperature data, fluid parameters of exhaust gases and cooling water, geometrical features, and material properties of the TEG system. According to these known parameters, it is required to calculate the output parameters of the TEG system, such as output power and conversion efficiency.

The given temperature data include the inlet exhaust temperature (T_{exi}), inlet water temperature (T_{wai}), outlet exhaust temperature (T_{exo}), and outlet water temperature (T_{wao}), which can be measured by using thermocouples. However, in the case of theoretical analysis, it is usually necessary to predict the performance of the automotive TEG system under the given inlet air temperature (T_{exi}) and inlet water temperature (T_{wai}), while the outlet exhaust temperature (T_{exo}) and outlet water temperature (T_{wao}) can not be known. The modeling approaches of these two cases are described respectively as follows:

Under the given T_{exi}, T_{wai}, T_{exo}, and T_{wao}, the amount of heat transfer between exhaust gases and heat exchanger, and between cooling water and heat sink can be expressed by Eq. (51) and Eq. (52), respectively.

$$Q_{\mathrm{h}} = h_{\mathrm{ex}} A_{\mathrm{eff}} \left(T_{\mathrm{ex}} - T_{\mathrm{h\_iw}} \right) \tag{51}$$

$$Q_{\mathrm{c}} = h_{\mathrm{wa}} A_{\mathrm{sink}} \left(T_{\mathrm{c\_iw}} - T_{\mathrm{wa}} \right) \tag{52}$$

with

$$T_{\mathrm{ex}} = \frac{T_{\mathrm{exi}} + T_{\mathrm{exo}}}{2} \tag{53}$$

$$T_{\mathrm{wa}} = \frac{T_{\mathrm{wai}} + T_{\mathrm{wao}}}{2} \tag{54}$$

where, h_{ex} and h_{wa} are the convective heat transfer coefficients of exhaust gases and water respectively. A_{eff} is the effective contact area between exhaust gases and the heat exchanger. A_{sink} is the contact area between cooling water and heat sink. $T_{\mathrm{h\_iw}}$ is the inner wall temperature of the heat exchanger. $T_{\mathrm{c\_iw}}$ is the inner wall temperature of the heat sink.

To compute convective heat transfer coefficients of h_{ex} and h_{wa}, empirical formulas are commonly used. Considering the different flow patterns of exhaust gases and cooling water, different empirical formulas can be used to minimize the error [87]. For exhaust gases, the mean Nusselt number can be estimated by the Gnielinski correlation, which is:

$$\mathrm{Nu} = \frac{(f/8)(\mathrm{Re}-1000)\mathrm{Pr}}{1+12.7\sqrt{f/8}\left(\mathrm{Pr}^{2/3}-1\right)} \tag{55}$$

with

$$f = \left(1.82 \lg \mathrm{Re} - 1.64\right)^{-2} \tag{56}$$

For cooling water, its mean Nusselt number can be obtained by the Dittus-Boelter correlation, which is:

$$\mathrm{Nu} = 0.023 \mathrm{Re}^{0.8} \mathrm{Pr}^{0.4} \tag{57}$$

In Eqs (55), (56) and (57), the Reynold number (Re) and Prandtl number (Pr) can be expressed as:

$$\mathrm{Re} = \frac{\rho v D}{\mu} \tag{58}$$

$$\mathrm{Pr} = \frac{\mu c}{\lambda} \tag{59}$$

with

$$v = \frac{\dot{m}}{\rho A} \tag{60}$$

$$D = \frac{4A}{L} \tag{61}$$

where, ρ is the fluid density, v is the fluid velocity, D is the hydraulic diameter, μ is the dynamic viscosity of fluids, c is the specific heat of fluids, λ is the thermal conductivity of fluids, $\dot{m}$ is the mass flow rate of fluids, A is the cross-sectional area, and L is the wetted perimeter over the cross section.

Under the given mass flow rates of exhaust gases and cooling water, their Nusselt numbers can be calculated. And then, the convective heat transfer coefficient can be computed by:

$$h = \lambda \frac{\mathrm{Nu}}{D} \tag{62}$$

And then, the convective thermal resistances of exhaust gases ($R_{\mathrm{h\_conv}}$) and cooling water ($R_{\mathrm{c\_conv}}$) can be estimated by:

$$R_{\mathrm{h\_conv}} = \frac{1}{h_{\mathrm{ex}} A_{\mathrm{eff}}} \tag{63}$$

$$R_{\mathrm{c\_conv}} = \frac{1}{h_{\mathrm{wa}} A_{\mathrm{sink}}} \tag{64}$$

In which, A_{sink} can be directly obtained by the geometrical sizes of the heat sink. However, the situation of the heat exchanger is quite different. To effectively enhance the convective heat transfer between exhaust gases and the heat exchanger and improve the working temperature of the hot side of the TEG module, a fin structure is usually used in the heat exchanger to increase the contact area of convective heat transfer. The effective contact area is defined by:

$$A_{\mathrm{eff}} = A_{\mathrm{b}} + \eta_{\mathrm{fin}} A_{\mathrm{fin}} \tag{65}$$

with

$$\eta_{\mathrm{fin}} = \frac{\tanh\left(mH_{\mathrm{fin}}\right)}{mH_{\mathrm{fin}}} \tag{66}$$

$$m = \sqrt{\frac{2h_{\mathrm{ex}}}{\lambda_{\mathrm{fin}}\delta_{\mathrm{fin}}}} \tag{67}$$

where, A_{b} is the area of the base of the heat exchanger. η_{fin} , A_{fin}, H_{fin}, λ_{fin}, and δ_{fin} are the efficiency, area, height, thermal conductivity, and thickness of fins, respectively.

When the heat is transferred from the inner wall to the outer wall of the heat exchanger and heat sink, the conductive thermal resistances of the heat exchanger ($R_{\mathrm{h\_cond}}$) and heat sink ($R_{\mathrm{c\_cond}}$) can be defined by:

$$R_{\mathrm{h\_cond/c\_cond}} = \frac{\delta_{\mathrm{b/sink}}}{\lambda_{\mathrm{b/sink}} A_{\mathrm{b/sink}}} \tag{68}$$

where, δ and A are the thickness and cross-sectional area respectively. Subscripts sink and b denote heat sink and base of heat exchanger respectively.

When the heat moves from the heat exchanger (a bigger area) to the hot side of the TEG module (a smaller area), there is a constricted thermal resistance [88], which is defined by:

$$R_{\mathrm{cons}} = \frac{\varsigma\tau + 0.5\sqrt{\pi}\left(1-\varsigma\right)^{\frac{3}{2}} \cdot \Theta}{\lambda_{\mathrm{b}}\pi a} \tag{69}$$

with

$$\Theta = \frac{\tanh\left(\beta\tau\right) + \beta/\mathrm{Bi}}{1 + \left(\beta/\mathrm{Bi}\right)\tanh\left(\beta\tau\right)} \tag{70}$$

$$\varsigma = \frac{a}{b} = \frac{\sqrt{A_{ce}/\pi}}{\sqrt{A_b/\pi}} \tag{71}$$

$$\tau = \frac{\delta_{\mathrm{b}}}{b} \tag{72}$$

$$\beta = \pi + \frac{1}{\varsigma\sqrt{\pi}} \tag{73}$$

$$\mathrm{Bi} = \frac{1}{\pi\lambda_{\mathrm{b}} b R_{\mathrm{h\_conv}}} \tag{74}$$

When the heat moves from the cold side of the TEG module (a smaller area) to the heat sink (a bigger area), there is a spreading thermal resistance [88], which can be expressed as:

$$R_{\mathrm{sp}} = \frac{A_{\mathrm{sink}}^{0.5} - A_{\mathrm{ce}}^{0.5}}{\lambda_{\mathrm{sink}}\left(\pi A_{\mathrm{sink}} A_{\mathrm{ce}}\right)^{0.5}} \cdot \frac{\gamma\lambda_{\mathrm{sink}} A_{\mathrm{sink}} R_{\mathrm{wa}} + \tanh\left(\gamma\delta_{\mathrm{sink}}\right)}{1 + \gamma\lambda_{\mathrm{sink}} A_{\mathrm{sink}} R_{\mathrm{wa}} \cdot \tanh\left(\gamma\delta_{\mathrm{sink}}\right)} \tag{75}$$

with

$$\gamma = \frac{\pi^{\frac{3}{2}}}{A_{\text{sink}}^{0.5}} + \frac{1}{A_{ce}^{0.5}} \tag{76}$$

In addition, the conductive thermal resistances of the hot side ($R_{\text{h\_ce}}$) and cold side ($R_{\text{c\_ce}}$) ceramic plates can be estimated by Eq. (77). Generally, the area of the hot side ceramic plate is equal to that of the cold side ceramic plate, which is $A_{\text{h\_ce}}=A_{\text{c\_ce}}$.

$$R_{\text{h\_ce/c\_ce}} = \frac{\delta_{\text{ce}}}{\lambda_{\text{ce}} A_{\text{h\_ce/c\_ce}}} \tag{77}$$

Similarly, the conductive thermal resistances of the hot side ($R_{\text{h\_co}}$) and cold side ($R_{\text{c\_co}}$) of copper electrodes can be estimated by Eq. (78), and $A_{\text{h\_co}}$ is generally equal to $A_{\text{c\_co}}$.

$$R_{\text{h\_co/c\_co}} = \frac{\delta_{\text{co}}}{\lambda_{\text{co}} A_{\text{h\_co/c\_co}}} \tag{78}$$

As described above, all thermal resistances from exhaust gases to the hot side of thermoelectric legs and from the cold side of thermoelectric legs to cooling water are modeled completely. And thus, the total hot side and cold side thermal resistances of R_{h} and R_{c} can be defined by:

$$R_{\text{h}} = R_{\text{h\_conv}} + R_{\text{h\_cond}} + R_{\text{cons}} + R_{\text{h\_ce}} + R_{\text{h\_co}} \tag{79}$$

$$R_{\text{c}} = R_{\text{c\_conv}} + R_{\text{c\_cond}} + R_{\text{sp}} + R_{\text{c\_ce}} + R_{\text{c\_co}} \tag{80}$$

Finally, the overall hot side heat flux and cold side flux can be expressed as:

$$Q_{\text{h}} = \frac{T_{\text{ex}} - T_{\text{h\_leg}}}{R_{\text{h}}} = \alpha_{\text{pn}} I T_{\text{h\_leg}} + \frac{T_{\text{h\_leg}} - T_{\text{c\_leg}}}{R_{\text{leg}}} - \frac{1}{2} I^2 R_{\text{in}} \tag{81}$$

$$Q_{\text{c}} = \frac{T_{\text{c\_leg}} - T_{\text{wa}}}{R_{\text{c}}} = \alpha_{\text{pn}} I T_{\text{c\_leg}} + \frac{T_{\text{h\_leg}} - T_{\text{c\_leg}}}{R_{\text{leg}}} + \frac{1}{2} I^2 R_{\text{in}} \tag{82}$$

Therefore, the output power of the TEG module can be estimated by:

$$P = Q_{\text{h}} - Q_{\text{c}} \tag{83}$$

The electric current can be expressed as:

$$I = \frac{\alpha_{\text{pn}} \left(T_{\text{h\_leg}} - T_{\text{c\_leg}} \right)}{R_{\text{in}} + R_{\text{L}}} \tag{84}$$

According to Eqs (81)-(84), there are six formulas with six unknowns of Q_{h}, Q_{c}, $T_{\text{h\_leg}}$, $T_{\text{c\_leg}}$, P, and I. Ultimately, the output power of the automotive TEG system can be computed, and the conversion efficiency is equal to the output power divided by the hot side heat flux, that is:

$$\eta = \frac{P}{Q_{\text{h}}} \tag{85}$$

In addition, by using the iterative method described in Fig. 4, the temperature-dependent thermoelectric material properties can be taken into consideration, which can further improve the reasonability of this model.

However, when T_{exo} and T_{wao} are not given, Eqs (81)-(84) can not solve eight unknowns of Q_h, Q_c, T_{exo}, T_{wao}, T_{h_leg}, T_{c_leg}, P, and I, and two additional equations are needed. For this reason, the overall heat flux of the hot side and cold side can also be characterized by the change of internal energy of exhaust gases and cooling water, which are:

$$Q_{\mathrm{h}} = c_{\mathrm{ex}} \dot{m}_{\mathrm{ex}} \left(T_{\mathrm{exi}} - T_{\mathrm{exo}} \right) \tag{86}$$

$$Q_{\mathrm{c}} = c_{\mathrm{wa}} \dot{m}_{\mathrm{wa}} \left(T_{\mathrm{wao}} - T_{\mathrm{wai}} \right) \tag{87}$$

Based on the above analysis, the performance of the automotive TEG system can be evaluated with given temperature data, fluid parameters, geometric characteristics, and material properties. In Ref. [89], under the condition of neglecting the thermal resistances (R_h and R_c) and taking the exhaust gas temperature (T_{ex}) and cooling water temperature (T_{wa}) as the working temperature of the hot side and cold side of the TEG module directly, the thermal resistance-based analytical model of automotive TEG system was divided into different submodels according to different leg rows along the direction of exhaust gas downward flow. The submodels were computed by using engineering equation solver (EES) software. According to model results, a TEG module composed of Mg_2Si/Zn_4Sb_3 for high-temperature regions followed by Bi_2Te_3 for low-temperature regions was optimized by the authors.

With the consideration of convective and conductive thermal resistances, Wang et al. [90], Vale et al. [91], Mostafavi and Mahmoudi [92], and Marvão et al. [93] used the thermal resistance-based analytical model to evaluate the performance of automotive TEG system and to study the effects of exhaust mass flow rate, exhaust temperature, geometry size of fins and heat exchanger on the performance. Some useful findings were obtained in their research. Furthermore, the thermal resistance-based analytical model of the automotive TEG system was improved in Refs [87, 88] by considering the constricted thermal resistance (R_{cons}) and spreading thermal resistance (R_{sp}). However, the temperature dependence of thermoelectric material properties was omitted in Refs [88, 90, 92], or the average temperature of the hot side (T_{h_leg}) and cold side (T_{c_leg}) of TEG legs was adopted to evaluate the thermoelectric properties in Refs [87, 91, 93]. Therefore, the accuracy of the developed models can be further improved by using reasonable methods to deal with the temperature-dependent thermoelectric properties.

The thermal resistance-based analytical model can also be used to evaluate the performance of some novel TEG system structures. Zhao et al. [94, 95] proposed an intermediate fluid TEG system in which the exhaust waste heat is transferred by boiling and condensation of the intermediate fluid. Combined with the heat transfer analysis of the intermediate fluid, the output performance of the TEG system for automotive exhaust waste heat recovery was studied by using the thermal resistance-based analytical model. The results indicated that the peak output power of the proposed structure is significantly higher than that of the traditional structure. In addition, the model can be used to predict the performance of the TEG system with phase change materials [96].

In other fields of waste heat recovery, Meng et al. [7] utilized the thermal resistance-based analytical model to evaluate the performance of the TEG system for waste heat recovery from industrial gas, while ignoring the constricted and spreading thermal resistances and using constant thermoelectric material properties. Kristiansen et al. [97] constructed a TEG system to recover waste heat from a marine waste incinerator and used the thermal resistance-based analytical model to optimize the parameters of the heat exchanger and TEG module. The convective, conductive, and spreading thermal resistances (R_{h_conv}, R_{c_conv}, R_{h_cond}, R_{c_cond}, R_{h_ce}, R_{c_ce}, and R_{sp}) were considered in their theoretical analysis. The basic equations in Refs [7, 97] are consistent with those of the thermal resistance-based analytical model of the automotive TEG system.

On the other hand, the temperature and mass flow rate of automotive exhaust gas will change with the change in vehicle operating conditions. The steady-state performance analysis of the automotive TEG system can not reveal its dynamic response characteristics. Based on the temperature and mass flow rate data of exhaust gas at different time points, Gou et al. [98] and Lan et al. [99] used the thermal resistance-based analytical model to evaluate the dynamic performance of the TEG system applied to waste heat recovery. However, according to the transient numerical simulation of the TEG module [58], it can be observed that the transient response of output power and conversion efficiency has an obvious time delay phenomenon, which can not be considered by the thermal resistance model. Besides, when considering the transient fluid flow and heat transfer in fluid regions, the time delay may be more obvious, which leads to the larger error of the transient performance predicted by the thermal resistance-based analytical model of the TEG system for fluid waste heat recovery.

Table 2. Lists of recent thermal resistance-based analytical models of TEG system applied in fluid waste heat recovery.

Steady/transient state	Thermal resistances in consideration	Temperature-dependent thermoelectric properties	Sources
Steady state	No	Using constant thermoelectric material properties	[89]
Steady state	R_{h_conv}, R_{c_conv}, R_{h_cond}, R_{c_cond}	Using constant thermoelectric material properties	[92, 94, 95]
Steady state	R_{h_conv}, R_{c_conv}, R_{h_cond}, R_{c_cond}, R_{h_ce}, R_{c_ce},	Using constant thermoelectric material properties	[7]
Steady state	R_{h_conv}, R_{c_conv}, R_{h_cond}, R_{c_cond},	Using constant thermoelectric material	[97]

	R_{sp}, R_{h_ce}, R_{c_ce},	properties	
Steady state	R_{h_conv}, R_{c_conv}, R_{h_cond}, R_{c_cond}, R_{h_ce}, R_{c_ce}, R_{h_co}, R_{c_co}	Using constant thermoelectric material properties	[90, 96]
Steady state	R_{h_conv}, R_{c_conv}, R_{h_cond}, R_{c_cond}, R_{h_ce}, R_{c_ce}, R_{h_co}, R_{c_co}	Evaluated by using the average temperature of the hot side and cold side of TEG legs	[91, 93]
Steady state	R_{h_conv}, R_{c_conv}, R_{h_cond}, R_{c_cond}, R_{cons}, R_{sp}, R_{h_ce}, R_{c_ce}	Using constant thermoelectric material properties	[88]
Steady state	R_{h_conv}, R_{c_conv}, R_{h_cond}, R_{c_cond}, R_{cons}, R_{sp}, R_{h_ce}, R_{c_ce}, R_{h_co}, R_{c_co}	Evaluated by using the average temperature of the hot side and cold side of TEG legs	[87]
Steady state	R_{h_conv}, R_{c_conv}, R_{h_cond}, R_{c_cond}, R_{cons}, $R_{h\ ce}$, $R_{c\ ce}$, $R_{h\ co}$, $R_{c\ co}$	Evaluated by using an iterative method	[25]
Transient state using the data at different time points	R_{h_conv}, R_{c_conv}, R_{h_cond}, R_{c_cond}, R_{h_ce}, R_{c_ce}, R_{h_co}, R_{c_co}	Using constant thermoelectric material properties	[98]
Transient state using the data at different time points	R_{h_conv}, R_{c_conv}, R_{h_cond}, R_{c_cond}, R_{h_ce}, R_{c_ce}, R_{h_co}, R_{c_co}	Evaluated by using the average temperature of the hot side and cold side of TEG legs	[99]

Recent developed thermal resistance-based analytical models of the TEG system applied in fluid waste heat recovery are tabulated in Table 2. In order to ensure high enough model accuracy, the thermal resistances of R_{h_conv}, R_{c_conv}, R_{h_cond}, R_{c_cond}, R_{h_ce}, R_{c_ce} are required to be comprehensively considered, because the temperature changes greatly when the heat is transferred through these thermal resistances. Due to the high thermal conductivity and small thickness of copper electrodes, ignoring the conductive thermal resistances of R_{h_co} and R_{c_co} has little effect on the output performance, and thus, the conductive thermal resistance of copper electrodes is ignored in a considerable number of studies. The value of constricted and spreading thermal resistances is depended on the area difference between the TEG module and contact surfaces of the heat exchanger and heat sink. When the area of the hot side surface of the heat exchanger and cold side surface of the heat sink is larger than the cross-sectional area of the ceramic plate, the corresponding thermal resistances of R_{cons} and R_{sp} should not be neglected, and vice versa. In addition, the thermoelectric material properties are highly temperature-dependent and nonlinear, therefore, appropriate methods should be adopted to ensure reasonability.

However, the thermal resistance-based analytical model is based on the assumption that there is no heat loss between the TEG system and the surrounding environment, and there is no Thomson heat along the TEG legs, which may lead to overestimation of output performance. The authors in Ref. [25] conducted a comparison between the thermal resistance-based analytical model and the fluid-thermal-electric multiphysics field coupled numerical model. Their results indicated that the numerical model is more reasonable than the thermal resistance model, and the accuracy of the thermal resistance model is highly affected by the exhaust temperature and mass flow rate. Details of the numerical model are introduced in the following sections.

3.2.2 CFD models

In general, the TEG system for fluid waste heat recovery is composed of a heat exchanger, TEG modules, heat sinks, and clamping devices. The heat exchanger is used to absorb heat from exhaust gases and transfer the heat to the hot side of TEG modules, and the heat transfer performance of the heat exchanger largely determines the output performance of the TEG system. The computational fluid dynamics (CFD) model is a common method to study and optimize the performance of heat exchangers, which is usually computed by using numerical analysis software such as ANSYS/Fluent and COMSOL. According to CFD results, temperature distributions of the whole TEG system and pressure distributions of fluids can be obtained. High hot side temperature, uniform hot side temperature distribution, and low pressure drop are key parameters to evaluate the performance of the heat exchanger. Besides, the obtained average surface temperature on both sides of TEG modules can be used to calculate the output performance of the TEG system through a simple calculation of Seebeck voltage. Furthermore, the average surface temperature can be used as the boundary conditions of the thermal resistance model and thermal-electric numerical model of the TEG module, and then more reasonable output performance can be predicted. These three methods based on the CFD model are introduced as follows:

i. CFD model only

The governing equations of the CFD model for the TEG system used to recover fluid waste heat include two parts: fluid regions and solid regions. In the fluid region of the exhaust channel and cooling water channel, the steady-state fluid flow follows the basic conservations of mass, momentum, and energy, which are:

$$\nabla \cdot \vec{v} = 0 \tag{88}$$

$$\nabla \cdot \left(\vec{v}\vec{v} \right) = -\frac{1}{\rho} \nabla p + \nabla \cdot \left(\mu \nabla \vec{v} \right) \tag{89}$$

$$\nabla \cdot \left(\lambda \nabla T \right) = \rho c \vec{v} \cdot \nabla T \tag{90}$$

where $\vec{v}$ is the fluid velocity vector. Eq. (88), Eq. (89), and Eq. (90) represent the mass, momentum, and energy conservations, respectively.

For the automotive TEG system, the flow pattern is usually turbulent and depended upon the Reynolds number. Two-equation turbulence models are the most commonly used methods to simulate the turbulent flow, including standard k - ε model, renormalization group (RNG) k - ε model, realizable k - ε model, and so on. Considering the high accuracy and high adaptivity of the RNG k - ε model, it has been widely adopted in previous studies [100, 101], which transport equations are:

$$\frac{\partial}{\partial t}(\rho k)+\frac{\partial}{\partial x_i}(\rho k u_i)=\frac{\partial}{\partial x_j}\left(\alpha_k \mu_{eff}\frac{\partial k}{\partial x_j}\right)+G_k+G_b-\rho\varepsilon-Y_M \tag{91}$$

$$\frac{\partial}{\partial t}(\rho \varepsilon)+\frac{\partial}{\partial x_i}(\rho \varepsilon u_i)=\frac{\partial}{\partial x_j}\left(\alpha_\varepsilon \mu_{eff}\frac{\partial \varepsilon}{\partial x_j}\right)+C_{1\varepsilon}\frac{\varepsilon}{k}\left(G_k+C_{3\varepsilon}G_b\right)-C_{2\varepsilon}\rho\frac{\varepsilon^2}{k}-R_\varepsilon \tag{92}$$

Detailed descriptions of the symbols in Eqs (91)-(92) can be found in the Fluent user's guide. The fluid flow and heat transfer in fluid regions can be completely worked out by Eqs (88)-(92). The heat is transferred between fluid regions and solid regions in the form of conjugate heat transfer, and the heat transfer in solid regions can be characterized by simple energy conservation, which is:

$$\nabla\cdot\left(\lambda\nabla T\right)=0 \tag{93}$$

Eqs (88)-(93) constitute the basic governing equations of the CFD model. By setting appropriate boundary conditions, the CFD model can be solved by numerical analysis software. For the automotive TEG system, the boundary conditions include inlet and outlet boundary conditions of exhaust gas and cooling water. In most research, the velocity inlet or mass flow rate inlet with constant inlet temperature is applied on the inlet surfaces of the fluid channel, while the pressure outlet is applied on the outlet surfaces. On the surfaces of the TEG system exposed to ambient air, the natural convective heat transfer boundary is defined. Ultimately, detailed fluid field and thermal field distribution characteristics of the TEG system are obtained. According to the average surface temperature on both sides of the TEG module, the output power can be expressed as:

$$P=\frac{\alpha_{\mathrm{pn}}\left(T_{\mathrm{h\_ce}}-T_{\mathrm{c\_ce}}\right)}{R_{\mathrm{in}}+R_{\mathrm{L}}} \tag{94}$$

In a great number of works, to reduce the numerical simulation time, the TEG module is usually simplified to a whole cube for CFD simulation, to obtain the temperature of the hot side and cold side of the ceramic plate. Furthermore, considering the heat transfer of all components of the TEG module, including ceramic plates, copper electrodes, and thermoelectric legs, the average surface temperature on both sides of the legs ($T_{\mathrm{h\_leg}}$ and $T_{\mathrm{c\_leg}}$) can be obtained, and then more reasonable output power can be calculated by replacing $T_{\mathrm{h\_ce}}$ and $T_{\mathrm{c\_ce}}$ with $T_{\mathrm{h\_leg}}$ and $T_{\mathrm{c\_leg}}$ respectively.

The optimization of the automotive TEG system mainly focuses on the improvement of the heat exchanger. The configuration of the fin structure in the heat exchanger increases the convective heat transfer area and the residual time of exhaust gas, thus increasing the temperature at the hot side of the heat exchanger, but the pressure drop will deteriorate. To balance the heat transfer performance and pressure drop, it is necessary to determine the appropriate fin parameters. Liu et al. [101] and Fernández-Yañez et al. [102] proposed several TEG system structures for automotive exhaust heat recovery, in which the heat exchanger adopts different fin designs. The authors used the CFD model to simulate the temperature and pressure distribution of the heat exchanger and studied the influence of different fin parameters on the performance of the heat exchanger, including fin angle, fin size, fin distribution, etc. Accordingly, some optimization design methods were put forward, which provide meaningful guidance for researchers to determine the appropriate fin structure.

In addition to fin structure, the parameters of the heat exchanger itself are also crucial to the performance of the TEG system. For a fixed exhaust pipe diameter, the heat exchanger can be designed with different aspect ratios. The oversized heat exchanger length will lead to a large temperature drop and pressure drop from inlet to outlet, and the oversized heat exchanger width will lead to low heat transfer performance for areas away from the center of the exhaust flow. For this reason, Kempf and Zhang [103] used the CFD model to analyze the thermal performance of the TEG system, and then studied the influence of heat exchanger material and various TEG configurations with six different TEG aspect ratios on the thermal performance. They reported that the optimal TEG aspect ratio increases with the thermal conductivity of heat exchanger material under a fixed number of TEG modules. Considering the space limitation of the vehicle exhaust system, Wan et al. [104] integrated a catalytic converter and muffler into the heat exchanger of the TEG system and studied its thermal performance through CFD simulation. Pacheco et al. [105] proposed a novel temperature-controlled TEG system concept in a light-duty vehicle, in which the novel heat exchanger consists of corrugated pipes embedded in the cast aluminum matrix and variable conductance heat pipes acting as spreaders of excess heat along the longitudinal direction. The performance of the novel heat exchanger is examined by the CFD model.

In Refs [101-105], the CFD model was only used to analyze the temperature and pressure characteristics of the TEG system, but not to calculate its output performance. According to the average surface temperature of the hot side and cold side of the TEG module predicted by the CFD model, the output power of the TEG system can be calculated by Eq. (94). Weng and Huang [106], Bai et al. [107], and Wang et al. [108, 109] proposed various TEG system configurations for vehicle exhaust waste heat recovery, and used this method to predict their output performance. Fig. 16 shows the temperature distribution on the hot side surface of the heat exchanger. The hot side working temperature of the TEG module can be obtained by evaluating its hot side average surface temperature. Similarly, the cold side working temperature can be obtained, so as to work out the output power of the TEG system. However, in the above literature, the TEG module was simplified as a whole cube to facilitate CFD simulations, which may lead to the overestimation of output power due to ignoring the thermal resistances of ceramic plates and copper electrodes. In addition, it is difficult to accurately express the equivalent material properties of the simplified TEG module. The model error caused by this factor can be avoided by considering the complete three-dimensional geometry of the TEG module in CFD simulation and using the average temperature of T_{h_leg} and T_{c_leg} to calculate the output power, although it requires more calculating power and time. Furthermore, the temperature dependence of thermoelectric material properties should be considered in CFD simulation to ensure that the results are more reasonable. On the other hand, the temperature distribution on the hot side of the TEG module is not uniform, and the working temperature difference among different thermoelectric legs is not consistent. The overall output current of the TEG module will be limited by the smallest one among legs because all legs are connected in series. Consequently, the use of average surface temperature will affect the model accuracy.

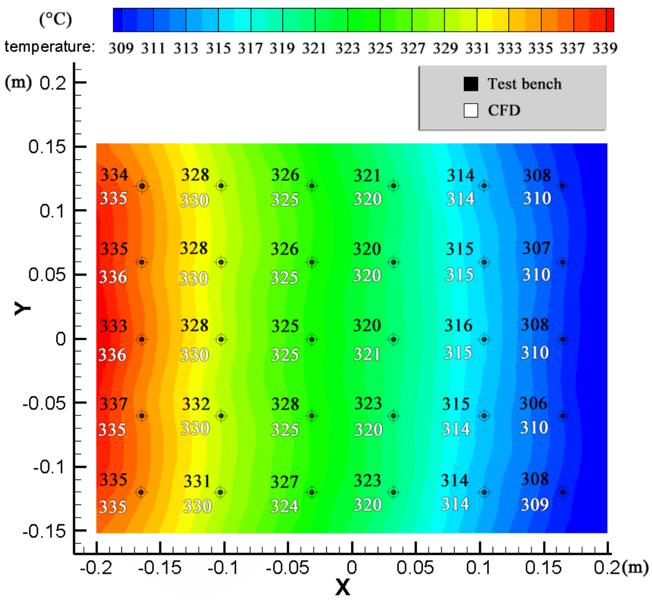

Fig. 16. The average hot-side temperature of the TEG module obtained by CFD [109].

ii. CFD model combined with thermal resistance model

After obtaining the average surface temperature of the hot side and cold side of the TEG module by the CFD model, taking the given temperature data as the boundary condition of the thermal resistance model of the TEG module, the output power and conversion efficiency of the TEG system can be calculated, which is a more reasonable method than using CFD model alone to predict the output performance of TEG system. Li et al. [110] combined the CFD model with the thermal resistance model of the TEG module to evaluate the performance of a fluid-based TEG system. The hot side and cold side temperature data were extracted from the CFD simulation, and the output performance of the TEG module was calculated by the thermal resistance model. In their study, both the complete three-dimensional geometry of the TEG module and the temperature dependence of thermoelectric materials were taken into account, which provides useful guidance for researchers to analyze the performance of the TEG system theoretically.

iii. CFD model combined with thermal-electric numerical model

Considering that the accuracy of the numerical model is higher than that of the thermal resistance model, the CFD model can also be combined with the thermal-electric numerical model of the TEG module to predict the output performance of the TEG system. Massaguer et al. [24] proposed a novel method to evaluate the fuel economy of the automotive TEG system, accounting for its output power, backpressure, weight, and coolant pumping power. The benefit of the TEG system applied to a vehicle was analyzed. In their work, firstly, the CFD simulation of the whole TEG system was completed by using ANSYS/Fluent, and the average temperature of the hot side and cold side of the TEG module was obtained, which was used as temperature boundary conditions of TEG module, and then the thermal-electric numerical simulation of the TEG module was completed by using ANSYS/Thermal-Electric, and the open-circuit output voltage of the module was obtained, which was used to predict the output power of TEG system. Their research provides a new idea for analyzing the potential of the TEG system in automotive waste heat recovery.

3.2.3 Fluid-thermal-electric multiphysics field coupled numerical models

In practice, the fluid field, thermal field, and electric field of the TEG system interact simultaneously. These three physical fields should be considered in the comprehensive numerical simulation of the TEG system. However, the CFD model can not consider the electric field, and the thermal-electric numerical model can not consider the fluid field. To accurately predict the performance of the TEG system for fluid waste heat recovery, it is necessary to establish a complete fluid-thermal-electric multiphysics field coupled numerical model. Also, it can be extended into a transient model to study the dynamic response characteristics of the TEG system under conditions of transient change in exhaust temperature and mass flow rate.

i. Steady state

For the steady-state fluid-thermal-electric multiphysics field coupled numerical model, its governing equations include Eqs (88)-(93) of the CFD model and Eqs (34)-(40) of the thermal-electric numerical model. Reddy et al. [111] integrated the source terms of the energy conservation equation of the TEG module into the energy conservation equation of the CFD model by using the user-defined scalar (UDS) function of Fluent. Combined with reasonable boundary conditions, a fluid-thermal-electric multiphysics field coupled numerical model of a simplified TEG system was established by the authors, and the output performance was predicted by the numerical simulation of Fluent. However, the simplified TEG system only contains one p-type TEG leg and one n-type TEG leg, which is far from the actual situation. The existing reports using Fluent/UDS to study the behavior of TEG devices or TEG systems are all based on a single thermoelectric couple. The reason for this is that the surfaces of each TEG leg need to be redefined by UDS, which means a huge workload for a TEG module, and it is easy to make human or software errors in the process of redefinition.

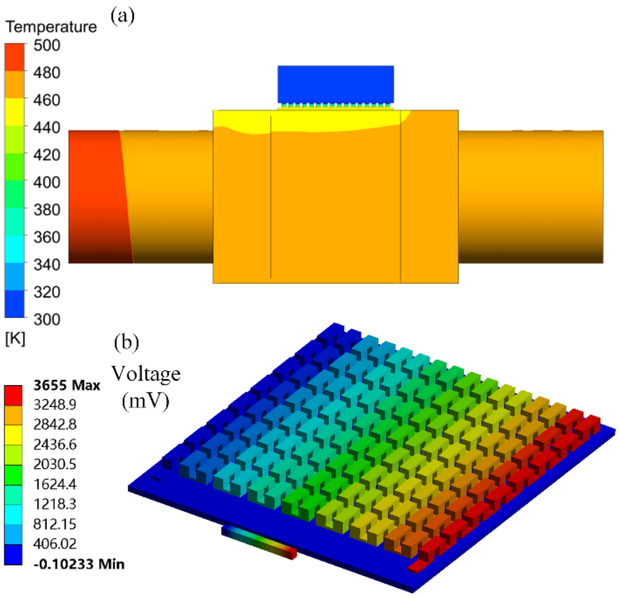

Fig. 17. Numerical results of a one-TEM-contained TEG system predicted by the fluid-thermal-electric multiphysics field coupled numerical model in Ref. [26]. (a) Temperature distribution of the whole TEG system. (b) Voltage distribution of the TEG module.

To extend the fluid-thermal-electric multiphysics field coupled numerical model from the simplified TEG system containing one single thermoelectric couple to a TEG system containing one TEG module, Luo et al. [23, 26] proposed a novel approach to solve the model via the coupling simulation of ANSYS/Fluent and ANSYS/Thermal-Electric. In their study, the CFD model was used to solve the primary temperature distribution of the TEG system, and the obtained temperature distribution of the TEG module was used as the temperature boundary condition of the thermal-electric numerical model to solve its electrical outputs. The obtained numerical results were shown in Fig. 17. Based on the numerical results, they proposed an effective optimization method to overcome the overall output current limitation of the TEG module due to uneven temperature distribution, in which, the length of each TEG leg was determined by its specific temperature difference.

In subsequent works [112, 113], Luo et al. further extended the fluid-thermal-electric multiphysics field coupled numerical model from a one-TEM-contained TEG system to a multiple-TEMs-contained TEG system. Similarly, in the numerical simulation, the temperature distribution of the hot side and cold side of TEG modules was used as the temperature boundary condition, and all TEG modules were set to be connected in series. A complete numerical simulation of the whole TEG system was reported for the first time, as shown in Fig. 18, which took into account the temperature dependence of thermoelectric materials and the topological relationship of load resistance. Different from the method of combining the CFD model with the thermal-electric numerical model, the thermal boundary condition loaded on both sides of TEG modules adopts temperature distribution in this model instead of average surface temperature. The influence of two modeling approaches on the output power of the TEG system was studied in Ref. [113], and the results showed that the output power predicted by average surface temperature is about 1% higher than that predicted by temperature distribution, which means the temperature distribution should not be ignored in predicting the output performance of TEG systems for fluid waste heat recovery.

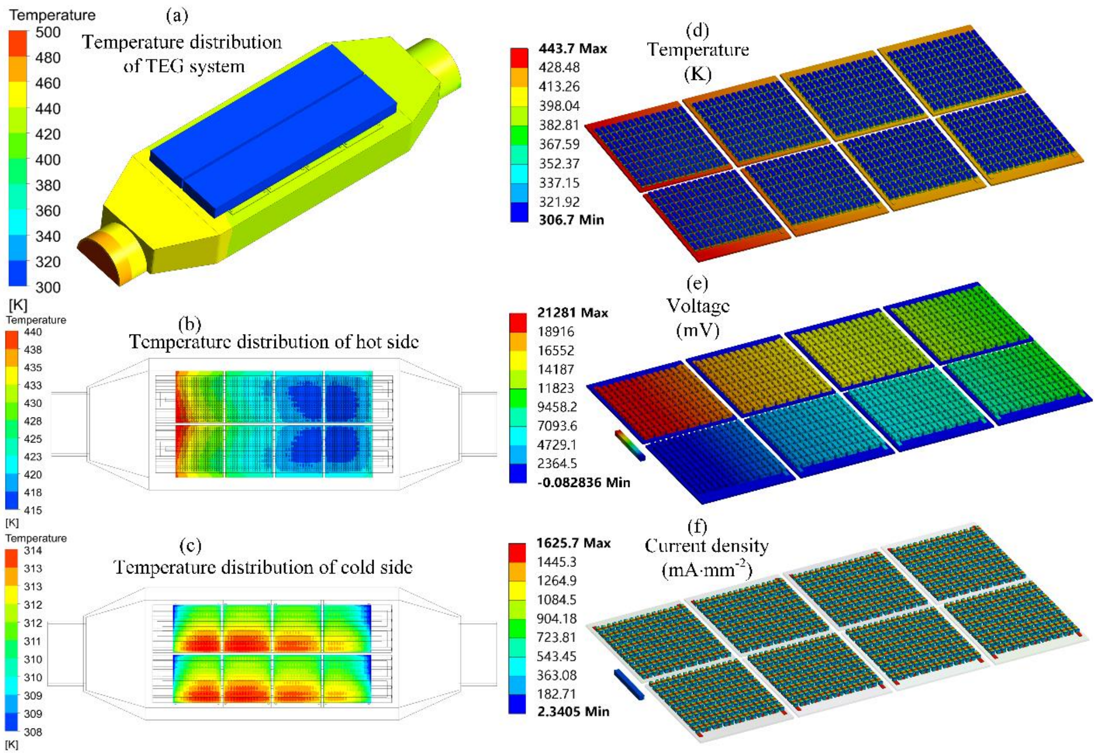

Fig. 18. Numerical results of multiple-TEMs-contained TEG system predicted by the fluid-thermal-electric multiphysics field coupled numerical model in Ref. [113]. (a) Temperature distribution of the whole TEG system. (b) Hot side temperature distribution of TEG modules. (c) Cold side temperature distribution of TEG modules. (d) Temperature distribution of TEG modules. (e) Voltage distribution of TEG modules. (f) Current density distribution of TEG modules.

However, the solution of the fluid-thermal-electric multiphysics field coupled numerical model by the coupling numerical simulation of ANSYS/Fluent and ANSYS/Thermal-Electric can not solve the fluid field, thermal field, and electric field at the same time. In this method, the fluid-thermal multiphysics coupled field is calculated first, and then the thermal-electric multiphysics coupled field is calculated. The influence of parasitic heat (including Joule heat and Peltier heat) generated by the thermoelectric effect on the thermal field and fluid field of the TEG system cannot be considered, which may cause additional model errors. A more reasonable solution needs to be developed.

By simplifying the TEG module with multiple TEG legs to a module containing only one pair of TEG legs, and assuming that the thermoelectric material properties were constant, Ma et al. [114] established a fluid-thermal-electric multiphysics field coupled numerical model to study the thermoelectric-hydraulic performance of a simplified TEG system. In their study, the fluid field, thermal field, and electric field were computed at the same time, and numerical simulations were performed on the COMSOL platform, as shown in Fig. 19(a). Compared with ANSYS, COMSOL has the advantages of multiphysics field coupled simulation, which can realize the complete simulation of a fluid-based TEG system. Considering the temperature dependence of thermoelectric materials, Yan et al. [115] studied the effect of heat exchanger channels with different cross-sectional shapes on the TEG system performance through the fluid-thermal-electric multiphysics field coupled numerical simulation on the COMSOL platform, as shown in Fig. 19(b). The research results showed that the TEG system with a rectangular-shaped channel can provide the highest output power and conversion efficiency. However, the cooling device was ignored and the cold side surfaces of TEG modules were directly set as a constant temperature in Ref. [115]. Besides, the load response characteristics were not considered in Refs [114, 115], and only the open-circuit voltage distribution was predicted.

To make the multiphysics numerical model closer to reality and with higher availability, Luo et al. [54] improved the model and used it to predict the performance of a TEG system containing one TEG module, taking into account the complete geometry of the TEG system, the temperature dependence of thermoelectric materials, and the topological connection of load resistance. Fig. 19(c) shows the temperature distribution of the whole TEG system and the voltage distribution of the TEG module. By comparing the numerical results of COMSOL coupled solver, COMSOL separate solver, and ANSYS, the influence of ignoring parasitic heat on the output performance of the TEG system was also studied. The prediction process of the COMSOL solver for TEG system performance was the same as that of ANSYS, wherein the fluid-thermal field was computed first, and then the thermal-electric field. It was reported that the neglect of parasitic heat will induce lower predictions of output performance and parasitic internal resistance, and an unreasonable prediction of maximum power point. The multiphysics model predicted by COMSOL coupled solver was more reasonable because the fluid field, thermal field, and electric field were calculated simultaneously. The research provides an effective method to predict the performance of the TEG system in fluid waste heat recovery, which can take all the actual conditions into account.

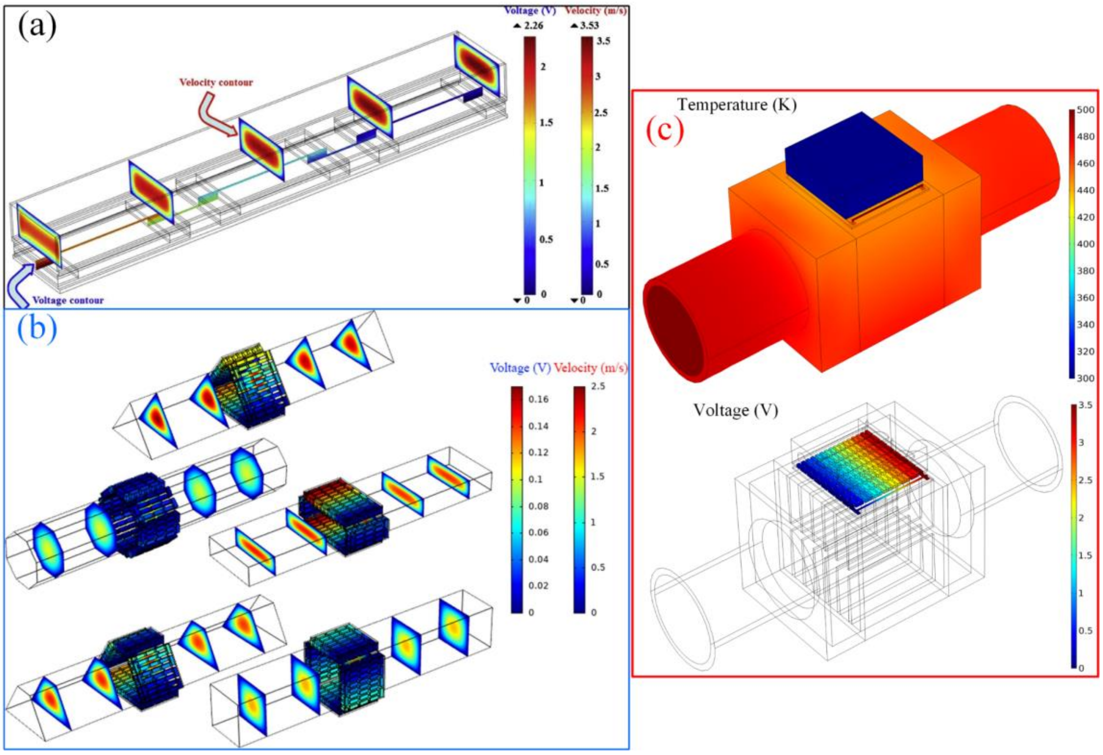

Fig. 19. Numerical results of the fluid-thermal-electric multiphysics field coupled numerical model obtained by COMSOL. (a) Velocity and voltage distributions of a simplified TEG system [114]. (b) Fluid velocity contour in channels and voltage distribution of TEG modules [115]. (c) Temperature distribution of the whole TEG system containing one TEG module and voltage distribution of the TEG module [54].

ii. Transient state

Furthermore, the COMSOL platform also provides a transient solver, which can be used to predict the dynamic response characteristics of the TEG system. However, ANSYS/Thermal-Electric can only conduct steady-state numerical simulations. Taking the previously developed TEG system as the research objective, Luo et al. [116] proposed a transient fluid-thermal-electric multiphysics field coupled numerical model and carried out the numerical simulation by COMSOL software. The transient governing equations of mass, momentum, and energy in the fluid region of the heat exchanger and heat sink channels can be expressed as:

$$\frac{\partial \rho}{\partial t}+\nabla \cdot\left(\rho \vec{v}\right)=0 \tag{95}$$

$$\frac{\partial}{\partial t}(\rho\vec{v})+\nabla\cdot(\rho\vec{v}\vec{v})=-\nabla p+\nabla\cdot\left[\mu\left(\nabla\vec{v}+\nabla\vec{v}^{T}\right)\right] \tag{96}$$

$$\rho c\frac{\partial T}{\partial t}+\rho c\vec{v}\cdot\nabla T-\nabla\cdot(\lambda\nabla T)=0 \tag{97}$$

where, t represents the time. Compared with the steady-state CFD model, the transient transport terms were included in the governing equations. Similarly, the k - ε model can be used to compute the turbulence flow of the fluid region, as represented in Eqs (91)-(92).

As for the solid region, including the heat exchanger, heat sink, and the whole TEG module, the transient energy conservation can be defined by:

$$(\rho c)_{\mathrm{m}}\frac{\partial T}{\partial t}=\nabla\cdot(\lambda_{\mathrm{m}}\nabla T)+\dot{S}_{\mathrm{m}} \tag{98}$$

where, subscript m represents different solid region materials. The first term denotes the transient term of internal energy change, the second term denotes the transient Fourier heat conduction, and the last term $\dot{S}_{\mathrm{m}}$ represents the energy source term. For different solid regions, the source term can be expressed as:

$$\dot{S}_{\mathrm{m}}=\begin{cases}\sigma_{\mathrm{p}}^{-1}(T)\vec{J}^{2}-T\vec{J}\cdot\nabla\alpha_{\mathrm{p}}(T)-\dfrac{\partial\alpha_{\mathrm{p}}(T)}{\partial T}T\vec{J}\cdot\nabla T_{\mathrm{p}}; & \text{p-type thermoelectric unit}\\ \sigma_{\mathrm{n}}^{-1}(T)\vec{J}^{2}-T\vec{J}\cdot\nabla\alpha_{\mathrm{n}}(T)-\dfrac{\partial\alpha_{\mathrm{n}}(T)}{\partial T}T\vec{J}\cdot\nabla T; & \text{n-type thermoelectric unit}\\ \sigma_{\mathrm{co}}^{-1}\vec{J}^{2}; & \text{copper}\\ \sigma_{\mathrm{L}}^{-1}\vec{J}^{2}; & \text{load resistance}\\ 0; & \text{heat exchanger, heat sink, and ceramic}\end{cases} \tag{99}$$

where, the energy source terms of p-type and n-type thermoelectric legs include Joule heat, Thomson heat, and Peltier heat. Since there is no Seebeck coefficient, only Joule heat is included in the source terms of copper electrodes and load resistance. For the heat exchanger, heat sink, and ceramic plates, there is no energy source because only Fourier heat conduction is involved.

The electric field conservation equations of the transient multiphysics numerical model are the same as those of the steady-state one, which are:

$$\vec{E}=-\nabla\phi+\alpha_{\mathrm{p,\,n}}(T)\nabla T \tag{100}$$

$$\vec{J}=\sigma_{\mathrm{m}}\vec{E} \tag{101}$$

$$\nabla\cdot\vec{J}=0 \tag{102}$$

Combined with transient thermal boundary conditions, such as transient exhaust temperature and transient mass flow rate, the dynamic response characteristics of a fluid-based TEG system can be predicted by numerical simulations on the COMSOL platform. To study the dynamic characteristics of the TEG system applied to vehicles, Luo et al. [116] first simulated the transient exhaust temperature and mass flow rate of a light-duty vehicle under seven Economic Commission of Europe (ECE) driving cycles through the vehicle simulation software of ADVISOR, as shown in Fig. 20 (c) and (d), and then used them as the transient boundary inputs of transient fluid-thermal-electric multiphysics field coupled numerical model of TEG system. Finally, the dynamic response characteristics of the TEG system were obtained by numerical simulation of COMSOL. Fig. 20 (e) shows the dynamic output voltage and output power, and Fig. 20 (f) shows the dynamic heat absorption and conversion efficiency. The authors performed the complete transient fluid-thermal-electric multiphysics field coupled numerical simulation for the first time, which provides an effective method to predict the dynamic performance of the TEG system.

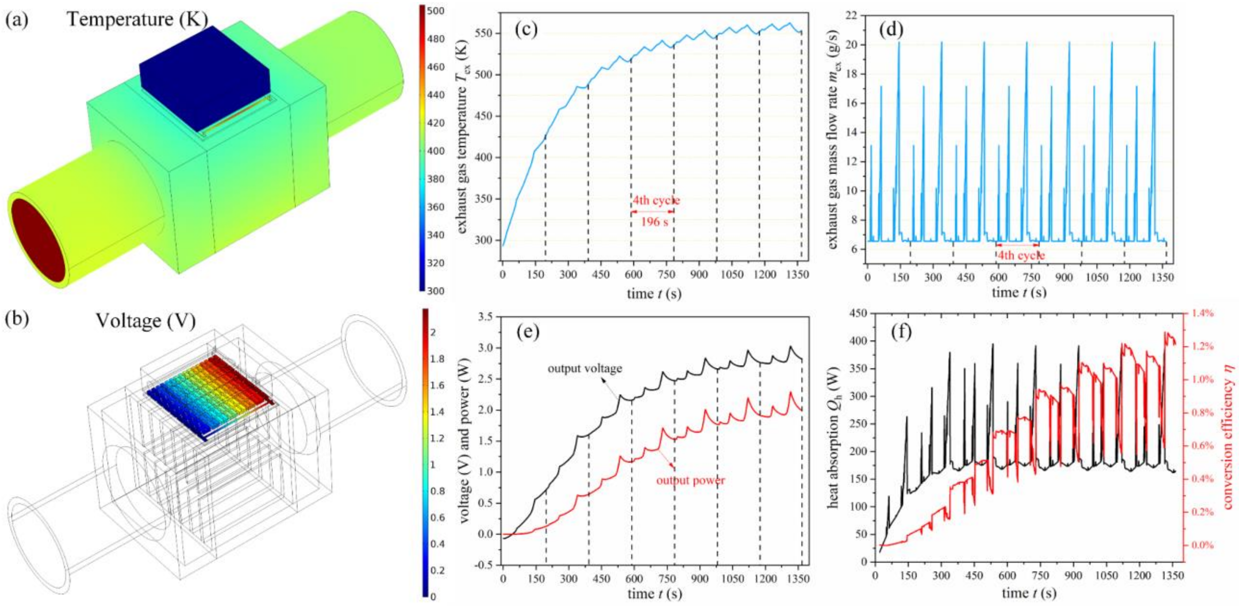

Fig. 20. Steady-state numerical results using the average exhaust parameters and transient characteristics of the TEG system [116]. (a) Temperature distribution and (b) voltage distribution of the whole TEG system predicted by the steady-state multiphysics numerical model. (c) Transient exhaust temperature and (d) transient exhaust mass flow rate under seven ECE driving cycles. (e) Dynamic output voltage and output power. (f) Dynamic heat absorption and conversion efficiency.

In previous studies, the output performance of an automotive TEG system under a complete driving cycle was usually predicted by steady-state performance analysis using average exhaust parameters. To analyze the performance difference between steady-state fluid-thermal-electric multiphysics filed coupled numerical model and transient one. Luo et al. [116] also predicted the steady-state performance under the conditions of average exhaust temperature and average exhaust mass flow rate of seven ECE cycles. Fig. 20 (a) and (b) show the temperature distribution and voltage distribution of the whole TEG system respectively. The steady-state numerical results were compared with transient numerical results. It was discovered that the total output power predicted by transient numerical simulation is 12.6% lower than that predicted by steady-state numerical simulation. Therefore, in practical situations, the transient fluid-thermal-electric multiphysics field coupled numerical model should be used to predict the dynamic performance of the TEG system, but not replaced by steady-state performance analysis. In addition, some meaningful findings were reported in their study, which brings a new perspective to the dynamic response characteristics of the TEG system.

3.2.4 Summary of numerical models for thermoelectric generator system

Section 3.2.2 and section 3.2.3 introduce the recent advances in the numerical model for TEG system applied to fluid waste heat recovery, from CFD models to complete fluid-thermal-electric multiphysics field coupled numerical models and from steady-state to transient state, as listed in Table 3. CFD model can accurately simulate the fluid flow in channels of the heat exchanger and heat sink. The heat exchanger is responsible for collecting heat from the hot fluid, and its performance determines the output performance of the entire TEG system. Therefore, the CFD model is widely used in thermal performance and pressure performance analysis of heat exchangers. According to the characteristics of temperature and pressure distribution predicted by the CFD model, the geometric parameters of the heat exchanger can be optimized.

Furthermore, the average surface temperature of the hot side and cold side of the TEG module predicted by the CFD model can be used as the temperature boundary conditions of the thermal resistance model and thermal-electric numerical model of the TEG module, and then the output performance of the TEG system can be estimated. In many studies, to reduce the execution time, the TEG module is simplified to a cube for CFD simulation. Generally, the CFD model combined with the numerical model can predict more reasonable results than the CFD model combined with the thermal resistance model. However, the temperature distribution on both sides of the TEG module is not uniform, and the output power predicted by the average surface temperature will be overestimated.

Consequently, based on the coupling simulation of ANSYS/Fluent and ANSYS/Thermal-Electric, a fluid-thermal-electric multiphysics field coupled numerical model is proposed, in which the temperature distribution of the TEG module is directly loaded on both sides of the TEG module to predict the output performance of TEG system. The established model can predict the output characteristics of the whole TEG system considering all actual conditions and has high accuracy. Nevertheless, this method first computes the fluid-thermal field and then the thermal-electric field, thus, the effect of parasitic heat (including Joule heat and Peltier heat) on the fluid-thermal field can not be considered.

There are two methods to solve the fluid field, thermal field, and electric field of the TEG system at the same time: one is to use the Fluent-UDS function to integrate the source term of the energy conservation equation into the CFD model; the other is to use professional multiphysics software of COMSOL to solve the fluid-thermal-electric multiphysics field coupled numerical model. On this basis, the numerical model for the fluid-based TEG system is further improved. However, it is difficult for Fluent-UDS to deal with the whole TEG module with multiple legs, and the research objective of existing reports mainly focuses on one pair of the thermoelectric leg. Unlike Fluent-UDS, COMSOL can perform the complete numerical simulation of the TEG system, which does not require any simplification and assumption.

On the other hand, the fluid-thermal-electric multiphysics field coupled numerical model can be extended from a steady state to a transient state on the COMSOL platform. In the field of automotive exhaust waste heat recovery, the research on the transient numerical analysis of TEG systems under transient driving cycles has been witnessed [116]. As well, the transient fluid-thermal-electric multiphysics field coupled numerical model can be used for the dynamic performance prediction of the TEG system in other application scenarios.

However, there is no report of transient numerical simulation using other numerical models. For the coupling simulation of ANSYS/Fluent and ANSYS/Thermal-Electric, it can not solve the transient fluid-thermal-electric multiphysics field coupled numerical model, because ANSYS/Thermal-Electric only provides a steady-state solver. For the CFD model, it can be used to conduct the transient CFD simulation, and the transient characteristics of the average surface temperature on both sides of the TEG module can be estimated. Furthermore, the transient output performance of the TEG system can be predicted by the thermal resistance model with temperature data under different time points, and predicted by the transient thermal-electric numerical model with higher accuracy. It is necessary to analyze the transient performance of the TEG system because the heat source is not static in an actual situation. Shortly, there may be a great number of studies on the dynamic performance of the TEG system using the above modeling approaches. Besides, some efforts need to be made to compare different transient numerical modeling methods to provide further guidance.

Table 3 Recent advances in numerical models for the TEG system applied to fluid waste heat recovery.

Model name	Steady state or transient state	Solver	Geometry and material simplifications	Features	Sources
CFD model only	Steady state	ANSYS/Fluent	• TEG module is	• performance analysis and	[101-

			simplified into a cube • constant thermoelectric properties	optimization for heat exchanger • no theoretical output performance prediction	105]
CFD model only	Steady state	ANSYS/Fluent	• TEG module is simplified into a cube • constant thermoelectric properties	• performance analysis and optimization for heat exchanger • output performance predicted by the average surface temperature difference	[106-109]
CFD model combined with thermal resistance model	Steady state	ANSYS/Fluent	• no geometry simplification • temperature-dependent thermoelectric properties	• using the average temperature of hot side and cold side TEG module predicted by CFD model as boundary conditions • output performance predicted by the thermal resistance model	[110]
CFD model combined with thermal-electric numerical model	Steady state	ANSYS/Fluent and ANSYS/Thermal-Electric	• TEG module is simplified into a cube in CFD simulation • temperature-dependent thermoelectric properties	• using the average temperature of hot side and cold side TEG module predicted by CFD model as boundary conditions • output performance predicted by the thermal-electric numerical model • can not take into account the temperature distribution	[24]
Fluid-thermal-electric multiphysics filed coupled numerical model	Steady state	ANSYS/Fluent combined with Fluent-UDS	• only one p-type leg and one n-type leg are included in the TEG module • temperature-dependent thermoelectric properties	• using Fluent-UDS to define the source terms of the energy conservation equation • difficult to handle the whole TEG module containing multiple legs	[111]
Fluid-thermal-electric multiphysics filed coupled numerical model	Steady state	ANSYS/Fluent and ANSYS/Thermal-Electric	• no geometry simplification • temperature-dependent thermoelectric properties	• using the temperature distribution of the TEG module predicted by the CFD model as boundary conditions of the thermal-electric numerical model • calculating the fluid-thermal field first and then the thermal-electric field • can not take into account the effect of parasitic heat on the fluid-thermal field	[23, 26, 112, 113]
Fluid-thermal-electric multiphysics filed coupled numerical model	Steady state	COMSOL	• only one p-type leg and one n-type leg are included in the TEG module • constant thermoelectric properties	• calculating the fluid field, thermal field, and electric field at the same time • open circuit • a complete multiphysics numerical model but with some assumptions	[114]
Fluid-thermal-electric multiphysics filed coupled numerical model	Steady state	COMSOL	• ignoring the heat sink and cooling source • temperature-dependent thermoelectric properties	• calculating the fluid field, thermal field, and electric field at the same time • open circuit • a complete multiphysics numerical model but with some	[115]

				assumptions	
Fluid-thermal-electric multiphysics filed coupled numerical model	Steady state	COMSOL	• no geometry simplification • temperature-dependent thermoelectric properties	• considering the load response characteristics • a complete multiphysics numerical model	[54]
Fluid-thermal-electric multiphysics filed coupled numerical model	Transient state	COMSOL	• no geometry simplification • temperature-dependent thermoelectric properties	• the firstly developed transient multiphysics numerical model • record high reasonability to predict the dynamic performance of the TEG system	[116]

4. Recommendations for the theoretical analysis of thermoelectric generation

4.1 Suggestions for improving model accuracy

The theoretical models for predicting the performance of TEGs include the thermal resistance model, numerical model, and analogy model. To improve the model accuracy, it is suggested to take into account the temperature-dependent thermoelectric material properties, including the Seebeck coefficient, thermal conductivity, and electrical resistivity. In detail, the thermal resistance model widely adopts the average temperature to evaluate the thermoelectric properties, however, this method may inevitably lead to errors because the thermoelectric properties are highly nonlinear. More reasonable methods, such as mentioned in Fig. 4, can make the thermal resistance model more accurate. Besides, the thermal resistances of ceramic plates and copper electrodes should not be ignored. The thermal-electric numerical model can accurately predict the output performance of TEGs. By introducing a load resistance into the circuit, the load response characteristics of TEGs can be studied, which is closer to the actual situation than the open circuit performance analysis. The analogy model is based on the basic equations of the thermal resistance model, and thus, the suggestions of the thermal resistance model are also applicable to the analogy model.

The theoretical models for predicting the performance of TEG systems can be grouped into two categories: TEG system directly contacted with the heat source and TEG system for fluid waste heat recovery. Similarly, the thermal resistance-based analytical model and thermal-electric numerical model are two commonly used methods to assess the performance of the TEG system directly contacted with the heat source. Both of them should consider the temperature-dependent thermoelectric material properties. For the thermal resistance-based analytical model, a complete thermal resistance network from the heat source to the hot side of the TEG module and from the cold side of the TEG module to the cooling source should be established. When heat is transferred from a larger cross-sectional area to a smaller cross-sectional area or from a smaller cross-sectional area to a larger cross-sectional area, the corresponding constricted thermal resistance and spreading thermal resistance should be integrated into the thermal resistance network. In the case of the thermal-electric numerical model, the complete geometry of the heat transfer unit between the heat (cooling) source and the TEG module should be considered in numerical simulation.

There are two theoretical models to predict the performance of the TEG system applied in fluid waste heat recovery: the thermal resistance-based analytical model and the numerical model. With the consideration of the factors mentioned above, the thermal resistance-based analytical model can exhibit high accuracy and reasonability. As for the numerical model, it includes the CFD model, CFD model combined with thermal resistance model, CFD model combined with a thermal-electric numerical model, and fluid-thermal-electric multiphysics field coupled numerical model. There is a great temperature drop from exhaust inlet to exhaust outlet, which leads to the change of material properties of exhaust gas. Therefore, the temperature-dependent material properties of both thermoelectric material and exhaust gas should be featured in the numerical simulation. In addition, geometry simplification is not recommended, because the temperature distribution plays a significant role in the output performance.

4.2 Usage of theoretical models in different scenarios

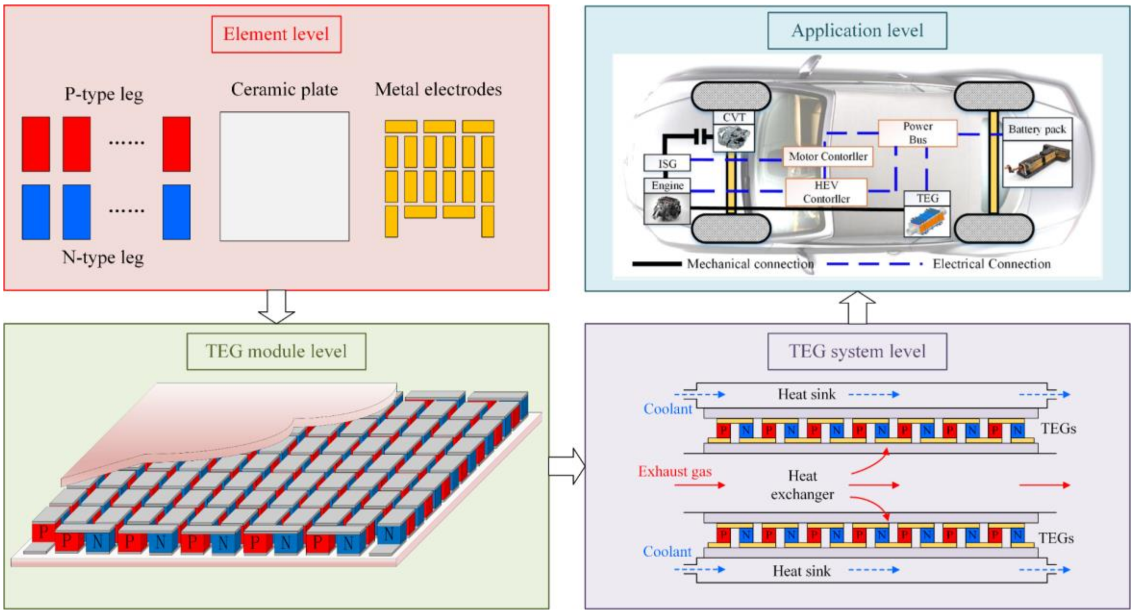

Fig. 21. The development process of the TEG system from element level to application level.

The application of thermoelectric generation technology in specific scenarios needs to go through four levels: element level, TEG module level, TEG system level, and application level, as shown in

Fig. 21. From the element level to the TEG module level, it is necessary to determine the optimal parameters of the thermoelectric leg, ceramic plate, and metal electrode, including material and geometrical parameters. To achieve this goal, the thermal resistance model and numerical model of the TEG module are widely adopted. Due to the unavoidable simplification and assumptions of the thermal resistance model, its model accuracy is worse than the numerical model. However, the thermal resistance model can quickly obtain the output performance under different parameters, which is suitable for the preliminary performance evaluation, structural design, and performance optimization of TEG components before manufacturing. The numerical model needs more calculation time than the thermal resistance model, but it can take all actual conditions into account. After the preliminary structural design of the TEG module is obtained, the numerical model can be used for further performance optimization to determine the final design scheme. The analogy model has the advantage of transient simulation and coupling simulation with the energy recovery circuit. It is suitable for the design and performance analysis of the energy recovery circuit, especially the maximum power point tracking (MPPT) circuit.

Similarly, from the TEG module level to the TEG system level, the thermal resistance-based analytical model is suitable for the preliminary performance analysis and structural design of the TEG system. Furthermore, to determine the optimal parameters and the final design schema of the TEG system, numerical models should be adopted to study the effect of different parameters on the output performance of the TEG system. For the TEG system applied in fluid waste heat recovery, the CFD model can be used to optimize both the thermal and pressure performance of the heat exchanger. However, CFD models are not recommended to be used to predict the performance of the TEG system under actual conditions, because the temperature distribution and other factors can not be considered in the CFD simulation. More accurately, the fluid-thermal-electric multiphysics field coupled numerical model should be used to predict the output characteristics, further optimize the performance, and determine the final design of the whole TEG system.

From the TEG system level to the application level, the transient characteristics of the heat source will affect the output performance of the TEG system. It is recommended to use the transient fluid-thermal-electric multiphysics field coupled numerical model to study the dynamic response characteristics of the TEG system under practical transient boundary conditions. And then, the obtained dynamic output voltage and output power can guide the use and the management of electricity produced by the TEG system.

5. Conclusions

In recent years, researchers have been developing theoretical models that can accurately predict the performance of thermoelectric generators (TEGs) and TEG systems. Compared with the experimental method, a reasonable theoretical model can reduce the cost of prototype development and save time. Therefore, the purpose of this work is to perform a comprehensive review of theoretical models in recent literature. TEG is the basic power generation unit of the TEG system, and the theoretical model of the TEG system can be regarded as an extension of the model of TEG. For this reason, the theoretical models of TEGs are reviewed first, and then the theoretical models of the TEG system.

With regards to the theoretical models of TEG, the thermal resistance model is the earliest used model to predict TEG performance, which is based on the balance of energy. By considering the temperature dependence of thermoelectric material and the thermal resistances of other components, the accuracy of the thermal resistance model can be further improved. However, the numerical model of TEG can take into account all actual conditions and predict more reasonable results than the thermal resistance model. In particular, some commercial finite element software programs, such as ANSYS and COMSOL, have integrated the governing equations of TEG into the software package, which promotes the utilization of numerical models among researchers. Moreover, based on the analogy between thermal circuit and electric circuit, the analogy model of TEG is developed on the platform of SPICE software. The analogy model facilitates the coupling simulation with the energy recovery circuit, which exhibits the potential use in the field of TEG recovery circuit development.

With regards to the theoretical models of TEG systems, they are classified into two groups: theoretical models of TEG systems directly contacted with heat source and theoretical models of TEG systems for fluid waste heat recovery. In the former case, the theoretical models of TEG can be applied to predict its performance by adding the thermal resistances and energy conservation equations of heat transfer units into the thermal resistance model and numerical model, respectively. In the case of the TEG system for fluid waste heat recovery, the thermal resistance-based analytical model can also be used to preliminarily evaluate the performance of the TEG system. To make the results more accurate, it is suggested to adopt the fluid-thermal-electric multiphysics field coupled numerical model.

On the other hand, different theoretical models have different application scenarios. Although numerical models can predict reasonable results, but suffer from the long execution time, especially for the TEG system applied in fluid waste heat recovery. On the contrary, thermal resistance models can quickly obtain the performance of TEG and TEG systems under different parameters. Therefore, thermal resistance models are suitable for preliminary performance evaluation, structural design, and performance optimization of TEGs and TEG systems before manufacturing. And numerical models of TEGs and TEG systems are suitable for further performance optimization to determine the final design scheme and the performance prediction under actual conditions. Moreover, the analogy model is convenient for the design of the energy recovery circuit, while the CFD model is suitable for the optimization of the heat exchanger. Combined with the advantages of each model, the development time of the TEG and TEG system can be shortened, and ensure optimal performance at the same time.

Finally, the transient thermal-electric numerical model of the TEG module and the transient fluid-thermal-electric multiphysics field coupled numerical model have been developed in recent research, which can take the dynamic characteristics of the heat source into account. The transient performance analysis of TEGs and TEG systems will remain a hot research field in the upcoming years.

Acknowledgments

This work was supported by the National Natural Science Foundation of China (51802261 and 52072217) and the Major Technological Innovation Project of Hubei Science and Technology Department (2019AAA164).

References

[1] Shen Z-G, Tian L-L, Liu X. Automotive exhaust thermoelectric generators: Current status, challenges and future prospects. Energy Convers Manage 2019;195:1138-73.

[2] Zhao Y, Fan Y, Li W, Li Y, Ge M, Xie L. Experimental investigation of heat pipe thermoelectric generator. Energy Convers Manage 2022;252:115123.

[3] Ge M, Zhao Y, Li Y, He W, Xie L, Zhao Y. Structural optimization of thermoelectric modules in a concentration photovoltaic–thermoelectric hybrid system. Energy. 2022;244:123202.

[4] Zhang Y. Thermoelectric Advances to Capture Waste Heat in Automobiles. ACS Energy Letters. 2018;3:1523-4.

[5] Crane D, LaGrandeur J, Jovovic V, Ranalli M, Adldinger M, Poliquin E, et al. TEG On-Vehicle Performance and Model Validation and What It Means for Further TEG Development. J Electron Mater 2013;42:1582-91.

[6] Luo Q, Li P, Cai L, Zhou P, Tang D, Zhai P, et al. A Thermoelectric Waste-Heat-Recovery System for Portland Cement Rotary Kilns. J Electron Mater 2015;44:1750-62.

[7] Meng F, Chen L, Feng Y, Xiong B. Thermoelectric generator for industrial gas phase waste heat recovery. Energy. 2017;135:83-90.

[8] O'Brien RC, Ambrosi RM, Bannister NP, Howe SD, Atkinson HV. Safe radioisotope thermoelectric generators and heat sources for space applications. J Nucl Mater 2008;377:506-21.
[9] LaLonde AD, Pei Y, Wang H, Jeffrey Snyder G. Lead telluride alloy thermoelectrics. Mater Today 2011;14:526-32.
[10] Kim SJ, We JH, Cho BJ. A wearable thermoelectric generator fabricated on a glass fabric. Energy Environ Sci 2014;7:1959-65.
[11] Li G, Zheng Y, Hu J, Guo W. Experiments and a simplified theoretical model for a water-cooled, stove-powered thermoelectric generator. Energy. 2019;185:437-48.
[12] Montecucco A, Siviter J, Knox AR. Combined heat and power system for stoves with thermoelectric generators. Appl Energy 2017;185:1336-42.
[13] Bell LE. Cooling, Heating, Generating Power, and Recovering Waste Heat with Thermoelectric Systems. Science. 2008;321:1457.
[14] Minnich AJ, Dresselhaus MS, Ren ZF, Chen G. Bulk nanostructured thermoelectric materials: current research and future prospects. Energy Environ Sci 2009;2:466-79.
[15] Zhang Q, Liao J, Tang Y, Gu M, Ming C, Qiu P, et al. Realizing a thermoelectric conversion efficiency of 12% in bismuth telluride/skutterudite segmented modules through full-parameter optimization and energy-loss minimized integration. Energy Environ Sci 2017;10:956-63.
[16] Zhang G, Fan L, Niu Z, Jiao K, Diao H, Du Q, et al. A comprehensive design method for segmented thermoelectric generator. Energy Convers Manage 2015;106:510-9.
[17] Lv H, Wang X-D, Meng J-H, Wang T-H, Yan W-M. Enhancement of maximum temperature drop across thermoelectric cooler through two-stage design and transient supercooling effect. Appl Energy 2016;175:285-92.
[18] Luo D, Wang R, Yu W, Zhou W. Parametric study of asymmetric thermoelectric devices for power generation. Int J Energy Res 2020:1-14.
[19] Bai S, Lu H, Wu T, Yin X, Shi X, Chen L. Numerical and experimental analysis for exhaust heat exchangers in automobile thermoelectric generators. Case Studies in Thermal Engineering. 2014;4:99-112.
[20] Lu X, Yu X, Qu Z, Wang Q, Ma T. Experimental investigation on thermoelectric generator with non-uniform hot-side heat exchanger for waste heat recovery. Energy Convers Manage 2017;150:403-14.
[21] Antonova EE, Looman DC. Finite elements for thermoelectric device analysis in ANSYS.

International Conference on Thermoelectrics2005. p. 215-8.
[22] Fraisse G, Ramousse J, Sgorlon D, Goupil C. Comparison of different modeling approaches for thermoelectric elements. Energy Convers Manage 2013;65:351-6.
[23] Luo D, Wang R, Yu W, Zhou W. Performance evaluation of a novel thermoelectric module with BiSbTeSe-based material. Appl Energy 2019;238:1299-311.
[24] Massaguer A, Massaguer E, Comamala M, Pujol T, González JR, Cardenas MD, et al. A method to assess the fuel economy of automotive thermoelectric generators. Appl Energy 2018;222:42-58.
[25] Luo D, Wang R, Yu W. Comparison and parametric study of two theoretical modeling approaches based on an air-to-water thermoelectric generator system. J Power Sources 2019;439:227069.
[26] Luo D, Wang R, Yu W, Zhou W. A novel optimization method for thermoelectric module used in waste heat recovery. Energy Convers Manage 2020;209:112645.
[27] Ando Junior OH, Maran ALO, Henao NC. A review of the development and applications of thermoelectric microgenerators for energy harvesting. Renewable Sustainable Energy Rev 2018;91:376-93.
[28] Chen W-H, Lin Y-X, Wang X-D, Lin Y-L. A comprehensive analysis of the performance of thermoelectric generators with constant and variable properties. Appl Energy 2019;241:11-24.
[29] Wu C. Analysis of waste-heat thermoelectric power generators. Appl Therm Eng 1996;16:63-9.
[30] Hsu C-T, Huang G-Y, Chu H-S, Yu B, Yao D-J. An effective Seebeck coefficient obtained by experimental results of a thermoelectric generator module. Appl Energy 2011;88:5173-9.
[31] Chen L, Li J, Sun F, Wu C. Performance optimization of a two-stage semiconductor thermoelectric-generator. Appl Energy 2005;82:300-12.
[32] Chen L, Li J, Sun F, Wu C. Effect of heat transfer on the performance of two-stage semiconductor thermoelectric refrigerators. J Appl Phys 2005;98:034507.
[33] Fan L, Zhang G, Wang R, Jiao K. A comprehensive and time-efficient model for determination of thermoelectric generator length and cross-section area. Energy Convers Manage 2016;122:85-94.
[34] Jincan C, Bihong L, Hongjie W, Guoxing L. Optimal design of a multi-couple thermoelectric generator. Semicond Sci Technol 2000;15:184.
[35] Liang X, Sun X, Tian H, Shu G, Wang Y, Wang X. Comparison and parameter optimization of a two-stage thermoelectric generator using high temperature exhaust of internal combustion engine. Appl Energy 2014;130:190-9.

[36] Reddy BVK, Barry M, Li J, Chyu MK. Mathematical modeling and numerical characterization of composite thermoelectric devices. Int J Therm Sci 2013;67:53-63.
[37] Luo D, Wang R, Yu W, Zhou W. Parametric study of a thermoelectric module used for both power generation and cooling. Renewable Energy 2020;154:542-52.
[38] Ebling D, Jaegle M, Bartel M, Jacquot A, Böttner H. Multiphysics Simulation of Thermoelectric Systems for Comparison with Experimental Device Performance. J Electron Mater 2009;38:1456-61.
[39] Bjørk R, Christensen DV, Eriksen D, Pryds N. Analysis of the internal heat losses in a thermoelectric generator. Int J Therm Sci 2014;85:12-20.
[40] Du C-Y, Wen C-D. Experimental investigation and numerical analysis for one-stage thermoelectric cooler considering Thomson effect. Int J Heat Mass Transfer 2011;54:4875-84.
[41] He H, Wu Y, Liu W, Rong M, Fang Z, Tang X. Comprehensive modeling for geometric optimization of a thermoelectric generator module. Energy Convers Manage 2019;183:645-59.
[42] Twaha S, Zhu J, Yan Y, Li B. A comprehensive review of thermoelectric technology: Materials, applications, modelling and performance improvement. Renewable Sustainable Energy Rev 2016;65:698-726.
[43] Jang B, Han S, Kim J-Y. Optimal design for micro-thermoelectric generators using finite element analysis. Microelectron Eng 2011;88:775-8.
[44] Wang X-D, Huang Y-X, Cheng C-H, Ta-Wei Lin D, Kang C-H. A three-dimensional numerical modeling of thermoelectric device with consideration of coupling of temperature field and electric potential field. Energy. 2012;47:488-97.
[45] Niu Z, Yu S, Diao H, Li Q, Jiao K, Du Q, et al. Elucidating modeling aspects of thermoelectric generator. Int J Heat Mass Transfer 2015;85:12-32.
[46] Chen M, Rosendahl LA, Condra T. A three-dimensional numerical model of thermoelectric generators in fluid power systems. Int J Heat Mass Transfer 2011;54:345-55.
[47] Meng J-H, Zhang X-X, Wang X-D. Characteristics analysis and parametric study of a thermoelectric generator by considering variable material properties and heat losses. Int J Heat Mass Transfer 2015;80:227-35.
[48] Chen W-H, Wu P-H, Lin Y-L. Performance optimization of thermoelectric generators designed by multi-objective genetic algorithm. Appl Energy 2018;209:211-23.
[49] Fan S, Gao Y. Numerical analysis on the segmented annular thermoelectric generator for waste heat recovery. Energy. 2019;183:35-47.

[50] Luo D, Wang R, Yu W, Zhou W. Parametric study of asymmetric thermoelectric devices for power generation. Int J Energy Res 2020;44:6950-63.

[51] Ming T, Wu Y, Peng C, Tao Y. Thermal analysis on a segmented thermoelectric generator. Energy. 2015;80:388-99.

[52] Wang R, Meng Z, Luo D, Yu W, Zhou W. A Comprehensive Study on X-Type Thermoelectric Generator Modules. J Electron Mater 2020.

[53] Hu X, Jood P, Ohta M, Kunii M, Nagase K, Nishiate H, et al. Power generation from nanostructured PbTe-based thermoelectrics: comprehensive development from materials to modules. Energy Environ Sci 2016;9:517-29.

[54] Luo D, Wang R, Yan Y, Sun Z, Zhou W, Ding R. Comparison of different fluid-thermal-electric multiphysics modeling approaches for thermoelectric generator systems. Renewable Energy 2021;180:1266-77.

[55] Yan Y, Malen JA. Periodic heating amplifies the efficiency of thermoelectric energy conversion. Energy Environ Sci 2013;6:1267-73.

[56] Meng J-H, Zhang X-X, Wang X-D. Dynamic response characteristics of thermoelectric generator predicted by a three-dimensional heat-electricity coupled model. J Power Sources 2014;245:262-9.

[57] Jia X-D, Wang Y-J, Gao Y-W. Numerical simulation of thermoelectric performance of linear-shaped thermoelectric generators under transient heat supply. Energy. 2017;130:276-85.

[58] Luo D, Yan Y, Wang R, Zhou W. Numerical investigation on the dynamic response characteristics of a thermoelectric generator module under transient temperature excitations. Renewable Energy 2021;170:811-23.

[59] Chavez JA, Ortega JA, Salazar J, Turo A, Garcia MJ. SPICE model of thermoelectric elements including thermal effects. Proceedings of the 17th IEEE Instrumentation and Measurement Technology Conference [Cat No 00CH37066]2000. p. 1019-23 vol.2.

[60] Chen M, Rosendahl LA, Condra TJ, Pedersen JK. Numerical Modeling of Thermoelectric Generators With Varing Material Properties in a Circuit Simulator. IEEE Trans Energy Convers 2009;24:112-24.

[61] Mitrani D, Salazar J, Turó A, García MJ, Chávez JA. One-dimensional modeling of TE devices considering temperature-dependent parameters using SPICE. Microelectron J 2009;40:1398-405.

[62] Fisac M, Villasevil FX, López AM. Design of a thermoelectric generator with fast transient response. Renewable Energy 2015;81:658-63.

[63] Mitrani D, Salazar J, Turó A, García MJ, Chávez JA. Transient distributed parameter electrical analogous model of TE devices. Microelectron J 2009;40:1406-10.

[64] Fraisse G, Lazard M, Goupil C, Serrat JY. Study of a thermoelement's behaviour through a modelling based on electrical analogy. Int J Heat Mass Transfer 2010;53:3503-12.

[65] Yilbas BS, Sahin AZ. Thermoelectric device and optimum external load parameter and slenderness ratio. Energy. 2010;35:5380-4.

[66] Zhang G, Jiao K, Niu Z, Diao H, Du Q, Tian H, et al. Power and efficiency factors for comprehensive evaluation of thermoelectric generator materials. Int J Heat Mass Transfer 2016;93:1034-7.

[67] Sandoz-Rosado E, Stevens R. Robust Finite Element Model for the Design of Thermoelectric Modules. J Electron Mater 2010;39:1848-55.

[68] Hu X, Takazawa H, Nagase K, Ohta M, Yamamoto A. Three-Dimensional Finite-Element Simulation for a Thermoelectric Generator Module. J Electron Mater 2015;44:3637-45.

[69] Liao M, He Z, Jiang C, Fan Xa, Li Y, Qi F. A three-dimensional model for thermoelectric generator and the influence of Peltier effect on the performance and heat transfer. Appl Therm Eng 2018;133:493-500.

[70] Lineykin S, Ben-Yaakov S. Modeling and Analysis of Thermoelectric Modules. IEEE Trans Ind Appl 2007;43:505-12.

[71] Champier D. Thermoelectric generators: A review of applications. Energy Convers Manage 2017;140:167-81.

[72] He W, Su Y, Riffat SB, Hou J, Ji J. Parametrical analysis of the design and performance of a solar heat pipe thermoelectric generator unit. Appl Energy 2011;88:5083-9.

[73] He W, Zhou J, Hou J, Chen C, Ji J. Theoretical and experimental investigation on a thermoelectric cooling and heating system driven by solar. Appl Energy 2013;107:89-97.

[74] Champier D, Bédécarrats JP, Kousksou T, Rivaletto M, Strub F, Pignolet P. Study of a TE (thermoelectric) generator incorporated in a multifunction wood stove. Energy. 2011;36:1518-26.

[75] Najjar YSH, Kseibi MM. Heat transfer and performance analysis of thermoelectric stoves. Appl Therm Eng 2016;102:1045-58.

[76] Nozariasbmarz A, Suarez F, Dycus JH, Cabral MJ, LeBeau JM, Öztürk MC, et al. Thermoelectric generators for wearable body heat harvesting: Material and device concurrent optimization. Nano Energy. 2020;67:104265.

[77] Suarez F, Nozariasbmarz A, Vashaee D, Öztürk MC. Designing thermoelectric generators for

self-powered wearable electronics. Energy Environ Sci 2016;9:2099-113.

[78] Liu K, Tang X, Liu Y, Xu Z, Yuan Z, Li J, et al. Preparation and optimization of miniaturized radioisotope thermoelectric generator based on concentric filament architecture. J Power Sources 2018;407:14-22.

[79] Khajepour A, Rahmani F. An approach to design a 90Sr radioisotope thermoelectric generator using analytical and Monte Carlo methods with ANSYS, COMSOL, and MCNP. Appl Radiat Isot 2017;119:51-9.

[80] Liu H-B, Meng J-H, Wang X-D, Chen W-H. A new design of solar thermoelectric generator with combination of segmented materials and asymmetrical legs. Energy Convers Manage 2018;175:11-20.

[81] Li P, Cai L, Zhai P, Tang X, Zhang Q, Niino M. Design of a Concentration Solar Thermoelectric Generator. J Electron Mater 2010;39:1522-30.

[82] Francioso L, De Pascali C, Sglavo V, Grazioli A, Masieri M, Siciliano P. Modelling, fabrication and experimental testing of an heat sink free wearable thermoelectric generator. Energy Convers Manage 2017;145:204-13.

[83] Liu Y, Shi Y, Li J, Guo X, Wang Y, Xiang Q, et al. Comprehensive performance prediction and power promotion for wearable thermoelectric generator with flexible encapsulation in practical application. Energy Convers Manage 2020;220:113080.

[84] Yang J, Stabler FR. Automotive Applications of Thermoelectric Materials. J Electron Mater 2009;38:1245-51.

[85] Zhang Y, Cleary M, Wang X, Kempf N, Schoensee L, Yang J, et al. High-temperature and high-power-density nanostructured thermoelectric generator for automotive waste heat recovery. Energy Convers Manage 2015;105:946-50.

[86] Risseh AE, Nee H-P, Goupil C. Electrical Power Conditioning System for Thermoelectric Waste Heat Recovery in Commercial Vehicles. IEEE Transactions on Transportation Electrification. 2018;4:548-62.

[87] Luo D, Wang R, Yu W, Sun Z, Meng X. Modelling and simulation study of a converging thermoelectric generator for engine waste heat recovery. Appl Therm Eng 2019;153:837-47.

[88] Hsiao YY, Chang WC, Chen SL. A mathematic model of thermoelectric module with applications on waste heat recovery from automobile engine. Energy. 2010;35:1447-54.

[89] Espinosa N, Lazard M, Aixala L, Scherrer H. Modeling a Thermoelectric Generator Applied to Diesel Automotive Heat Recovery. J Electron Mater 2010;39:1446-55.

[90] Wang Y, Dai C, Wang S. Theoretical analysis of a thermoelectric generator using exhaust gas of vehicles as heat source. Appl Energy 2013;112:1171-80.

[91] Vale S, Heber L, Coelho PJ, Silva CM. Parametric study of a thermoelectric generator system for exhaust gas energy recovery in diesel road freight transportation. Energy Convers Manage 2017;133:167-77.

[92] Mostafavi SA, Mahmoudi M. Modeling and fabricating a prototype of a thermoelectric generator system of heat energy recovery from hot exhaust gases and evaluating the effects of important system parameters. Appl Therm Eng 2018;132:624-36.

[93] Marvão A, Coelho PJ, Rodrigues HC. Optimization of a thermoelectric generator for heavy-duty vehicles. Energy Convers Manage 2019;179:178-91.

[94] Zhao Y, Wang S, Ge M, Liang Z, Liang Y, Li Y. Performance analysis of automobile exhaust thermoelectric generator system with media fluid. Energy Convers Manage 2018;171:427-37.

[95] Zhao Y, Wang S, Ge M, Liang Z, Liang Y, Li Y. Performance investigation of an intermediate fluid thermoelectric generator for automobile exhaust waste heat recovery. Appl Energy 2019;239:425-33.

[96] Catalan L, Araiz M, Aranguren P, Astrain D. Computational study of geothermal thermoelectric generators with phase change heat exchangers. Energy Convers Manage 2020;221:113120.

[97] Kristiansen NR, Snyder GJ, Nielsen HK, Rosendahl L. Waste Heat Recovery from a Marine Waste IncineratorUsing a Thermoelectric Generator. J Electron Mater 2012;41:1024-9.

[98] Gou X, Yang S, Xiao H, Ou Q. A dynamic model for thermoelectric generator applied in waste heat recovery. Energy. 2013;52:201-9.

[99] Lan S, Yang Z, Chen R, Stobart R. A dynamic model for thermoelectric generator applied to vehicle waste heat recovery. Appl Energy 2018;210:327-38.

[100] Niu Z, Diao H, Yu S, Jiao K, Du Q, Shu G. Investigation and design optimization of exhaust-based thermoelectric generator system for internal combustion engine. Energy Convers Manage 2014;85:85-101.

[101] Liu C, Deng YD, Wang XY, Liu X, Wang YP, Su CQ. Multi-objective optimization of heat exchanger in an automotive exhaust thermoelectric generator. Appl Therm Eng 2016;108:916-26.

[102] Fernández-Yañez P, Armas O, Capetillo A, Martínez-Martínez S. Thermal analysis of a thermoelectric generator for light-duty diesel engines. Appl Energy 2018;226:690-702.

[103] Kempf N, Zhang Y. Design and optimization of automotive thermoelectric generators for

maximum fuel efficiency improvement. Energy Convers Manage 2016;121:224-31.
[104] Wan Q, Liu X, Gu B, Bai W, Su C, Deng Y. Thermal and acoustic performance of an integrated automotive thermoelectric generation system. Appl Therm Eng 2019;158:113802.
[105] Pacheco N, Brito FP, Vieira R, Martins J, Barbosa H, Goncalves LM. Compact automotive thermoelectric generator with embedded heat pipes for thermal control. Energy. 2020;197:117154.
[106] Weng C-C, Huang M-J. A simulation study of automotive waste heat recovery using a thermoelectric power generator. Int J Therm Sci 2013;71:302-9.
[107] Bai W, Yuan X, Liu X. Numerical investigation on the performances of automotive thermoelectric generator employing metal foam. Appl Therm Eng 2017;124:178-84.
[108] Wang Y, Li S, Xie X, Deng Y, Liu X, Su C. Performance evaluation of an automotive thermoelectric generator with inserted fins or dimpled-surface hot heat exchanger. Appl Energy 2018;218:391-401.
[109] Wang Y, Li S, Zhang Y, Yang X, Deng Y, Su C. The influence of inner topology of exhaust heat exchanger and thermoelectric module distribution on the performance of automotive thermoelectric generator. Energy Convers Manage 2016;126:266-77.
[110] Li W, Peng J, Xiao W, Wang H, Zeng J, Xie J, et al. The temperature distribution and electrical performance of fluid heat exchanger-based thermoelectric generator. Appl Therm Eng 2017;118:742-7.
[111] Reddy BVK, Barry M, Li J, Chyu MK. Three-Dimensional Multiphysics Coupled Field Analysis of an Integrated Thermoelectric Device. Numerical Heat Transfer, Part A: Applications. 2012;62:933-47.
[112] Luo D, Wang R, Yu W, Zhou W. A numerical study on the performance of a converging thermoelectric generator system used for waste heat recovery. Appl Energy 2020;270:115181.
[113] Luo D, Wang R, Yu W, Zhou W. Performance optimization of a converging thermoelectric generator system via multiphysics simulations. Energy. 2020;204:117974.
[114] Ma T, Lu X, Pandit J, Ekkad SV, Huxtable ST, Deshpande S, et al. Numerical study on thermoelectric–hydraulic performance of a thermoelectric power generator with a plate-fin heat exchanger with longitudinal vortex generators. Appl Energy 2017;185:1343-54.
[115] Yan S-R, Moria H, Asaadi S, Sadighi Dizaji H, Khalilarya S, Jermsittiparsert K. Performance and profit analysis of thermoelectric power generators mounted on channels with different cross-sectional shapes. Appl Therm Eng 2020:115455.

[116] Luo D, Wang R, Yan Y, Yu W, Zhou W. Transient numerical modelling of a thermoelectric generator system used for automotive exhaust waste heat recovery. Appl Energy 2021;297:117151.